Bamboo Housing Structural Design

Francisco Barata Garcia

Dissertation to obtain the Master of Science Degree in

Civil Engineering

Supervisor: Prof. Luís Manuel Coelho Guerreiro

Examination Committee

Chairperson: Prof. Doutor Orlando José Barreiros D'Almeida Pereira

Supervisor: Prof. Doutor Luís Manuel Coelho Guerreiro

Member of the Committee: Prof. Doutor António Manuel Candeias de Sousa Gago

October 2021

Declaration

I declare that this document is an original work of my own authorship and that it fulfills all the requirements of the Code of Conduct and Good Practices of the Universidade de Lisboa.

Agradecimentos

Agradeço ao meu orientador, Professor Luís Guerreiro, a oportunidade de poder desenvolver esta dissertação de mestrado sob a sua orientação, tal como a sua disponibilidade e contribuição para o desenvolvimento da mesma.

Às pessoas envolvidas na Bamboo U, que com os seus projetos inovadores e cursos de excelência têm vindo a multiplicar continuamente a comunidade do bambu.

A todos os meus amigos, agradeço os momentos de descontração e convívio durante o desenvolvimento do trabalho, bem como o seu entusiasmo e interesse pelo tema.

À minha namorada, Carolina Alonzo Hill, agradeço toda a motivação, compreensão e carinho durante o desenvolvimento desta dissertação de mestrado.

À minha família, agradeço todo o suporte, confiança e preocupação ao longo de todas as fases do meu percurso académico.

À minha avó, a quem dedico este trabalho, por todo o apoio e amor que me deu toda a vida.

Resumo

O bambu é um material altamente sustentável com excelentes propriedades mecânicas, que começa a surgir como solução estrutural. Recentemente foram publicadas normas internacionais que regulam procedimentos de testagem, classificação e dimensionamento estrutural de bambu, que permitiram o desenvolvimento deste trabalho.

É apresentada informação bibliográfica sobre o material, de forma a entender as suas características, durabilidade e fiabilidade, necessárias à sua utilização. As ligações de bambu são também abordadas, referindo as dificuldades inerentes bem como as soluções propostas até à data.

Após expor os temas associados ao bambu que podem comprometer a sua utilização como elemento estrutural, é apresentado um caso prático que consiste no desenvolvimento de um projeto de uma estrutura residencial utilizando apenas bambu. A espécie Moso (*Phyllostachys edulis*) foi escolhida como base, e as suas características foram introduzidas no *software* onde foi modelada a estrutura. As ações consideradas seguiram as regras dos Eurocódigos e anexos nacionais. Foram comparadas as resistências calculadas pela norma internacional ISO 22156:2021 com as tensões devolvidas pelo programa. A resistência ao esforço transverso demonstrou ser mais reduzida do que as restantes, tal como a resistência à compressão caso o comprimento de encurvadura do elemento fosse significativo. As deformações foram também analisadas, e finalmente foi feita uma análise sísmica. Foram feitas modificações na estrutura de forma que todos os resultados apresentassem conformidade com as verificações. Esta dissertação sugere que o bambu é uma alternativa sustentável extremamente competente como elemento estrutural.

Palavras-Chave

Bambu Moso, Dimensionamento Estrutural, Estruturas em Bambu, Análise sísmica, Revisão bibliográfica

Abstract

The research presented examines several topics and concerns related to construction using bamboo, as well as the design of a bamboo structure. Bamboo is a functionally graded natural material that does not present uniform properties. Nevertheless, recent efforts in the standardization of grading, testing and structural design can overcome the anisotropy limitations. In regard to durability, treatments with boron provide a safe, economical, effective and sustainable way to make a structure last, as long as durability by design measures are performed. In connections, the hollow round shape and variable section of bamboo make joining members challenging, therefore more testing is required.

In the case study, a two-level structure using Moso bamboo was designed. The response forces were obtained from the model in the computer software and compared with allowable resistances calculated according to the structural design standard ISO 22156:2021. The loads and combinations follow the Eurocode guidelines and the Portuguese National Annex. The bamboo culms were modelled as hollow tubes with an outer diameter of 0,1 m and a wall thickness of 0,01 m. The allowable capacities calculated showed low shear resistance due to the tendency to split in the longitudinal direction, and the buckling capacity of the culms compromised the compressive capacity of the longer elements. However, no stress exceeded the resistances after alterations in the structure. The dynamic analysis results indicate that bamboo is exceedingly capable of resisting the earthquakes considered. This study suggests that bamboo design has notable potential as a sustainable, durable, seismically resistant housing alternative.

Keywords

Moso Bamboo, Bamboo Structural Design, Seismic analysis, Bamboo Literature Review, Standards

Table of Contents

List of Figures

List of Tables

List of Symbols

v_{b}	Basic wind velocity;
c_{dir}	Directional factor;
c_{season}	Season factor;
$v_{\mathrm{b},0}$	Fundamental value of the basic wind velocity;
c_r	Roughness factor;
z_0	Roughness length;
$z_{0,II}$	Roughness length in terrain category II;
c_{o}	Orography factor;
I_v	Turbulence intensity;
q_{p}	Peak velocity pressure;
q_{b}	Basic velocity pressure;
ρ	Air density;
w_e	Wind external pressure;
w_{i}	Wind internal pressure;
c_{pe}	External pressure coefficients;
c_{pi}	Internal pressure coefficients;
$R_{e,i}$	Reactions of element *i* under external loads;
$R_{i,i}$	Reactions of element *i* under internal loads;
A	Cross sectional area;
D	Outside diameter;
δ	Wall thickness;
I	Inertia;
E_{d}	Modulus of Elasticity design value;
E_k	Characteristic modulus of elasticity;
C_{DE}	Modification factor for service class and load duration;
C_T	Modification factor for service temperature;
f_i	Allowable design strength;
f_{ik}	Characteristic strength;
C_R	Member redundancy factor;
C_{DF}	Modification factor for service class and load duration;
FS_{m}	Material factor of safety;
f_c	Compression strength;
f_v	Shear strength;
f_t	Tension strength;
f_b	Bending strength;
N_{cr}	Compressive capacity;
P_{e}	Buckling capacity;

P_{c}	Crushing capacity;
C_{bow}	Reduction factor to account initial bow;
I_{min}	Minimum moment of inertia;
n	Number of culms;
K	Effective length coefficient;
L	L is the length of the element;
b_0	Maximum bow;
b_{max}	Maximum perpendicular distance from the centre of the culm cross section to the chord drawn from the centres of the ends of the piece of bamboo;
N_{cd}	Design compression force;
N_{td}	Design tensile force;
M_{cd}	Design bending force;
N_{tr}	Tensile resistance;
M_{r}	Bending resistance;
B	Moment amplification factor;
MOE	Modulus of Elasticity;

1. Introduction

1.1. Motivation

The construction industry accounts for 39% of the world's CO2 emissions (*World Green Building Council*, n.d.). Moreover, the increase in world population will create the need for sustainable housing alternatives. Building with bamboo can strongly contribute to the pressing need to combat climate change.

The global bamboo industry was valued at a market size of USD 68.8 billion in 2018, with an expectancy to grow at a compound annual growth rate of 5.0% from 2019 to 2025 (*Grand View Research*, n.d.). This is related to the diversity of products that bamboo can provide, contributing to circular economies that are congruent to many of the Sustainable Developments Goals laid by the United Nations.

As the fastest growing plant in the world, it can sequester 50 tons of CO2 per hectare per year, 3 times as much for the same area of timber planted (Walter Liese, 2015; *Bamboo U*, 2021; Rabik & Brown, 2004). Moreover, a single clump of bamboo can hold a tremendous amount of water and release it to the surrounding vegetation. Together with its extensive canopy that protects the land from extensive son exposure, bamboo can play an important part in restoring degraded land, preventing deforestation, controlling erosion and flooding.

Bamboo is harvested yearly, leaving the root system unharmed and continuingly producing more shoots (Asif, 2009). Therefore, it can also enable the communities that manage the life cycle of bamboo to thrive (e.g. *Environmental Bamboo Foundation*, n.d.)).

Acknowledging the advantages in regard to sustainability, this study's intention is to take a step towards demonstrating the capabilities of bamboo as a structural element. As an emerging material, there is still a shortage of scientific documents and data on topics related to building with bamboo. Nevertheless, recent efforts in standardizing tests, grading and structural design allow for regulated practices that will lead to making bamboo a conventional material. This dissertation suggests that bamboo design has notable potential as a sustainable, durable, seismically resistant housing alternative if considering seismic and durability design concerns.

1.2. Goals, Contributions and Structure

This work intends to firstly present a diverse state of the art, approaching topics that could possibly compromise the efficiency, safety or use of bamboo as a structural element. After providing a broader perspective through the literature review, a practical case is developed.

The case study demonstrates a static and dynamic analysis of a structure using bamboo as the only structural element. The structure is modelled in the computer software SAP2000 (*CSI Portugal | SAP2000*, n.d.), and the response forces are compared with the allowable resistances calculated according to the structural design standard ISO 22156:2021. The loads and combinations follow the recommendations of the Eurocode, as well as the national annex for the country of Portugal.

To implement this goal, the following tasks are required:

- Apprehend the state of the development of standards regarding bamboo;

- Describe the constitutional properties of bamboo to better understand its behaviour;
- Analyse the effects of different variables in the strength of bamboo;
- Approach subjects involved in the durability of bamboo (the causes of decay, applicable treatments available and the methods they imply, as well as the importance of seasoning and design awareness);
- Investigate the state of the art of connections of bamboo

In the process of performing load verifications of a bamboo structure, the underlying steps are:

- Select a bamboo species;
- Design the structure;
- Determine the loads the structure will be subjected to, as well as the load combinations;
- Take design assumptions of related to culm geometry and characteristic strengths;
- Calculate the design values of resistance to the different stresses;
- Compare the applied and allowable forces, and make modifications in the structure;
- Perform the dynamic analysis, analyse the stresses and consider alterations;

This text hopefully contributes both as a literature review document, synthesizing relevant topics, as well as an example of structural analysis according to the ISO 22156:2021 standard.

This dissertation is structured as follows: the present chapter presents the motivation and literature review; Chapter 2 introduces the constitution of the bamboo plant, as well as the variation of the material properties with age, density and moisture content; Chapter 3 focuses on the durability and treatments of bamboo, going through the causes of decay, treatment options and methods, seasoning, and how to design a structure considering the durability of bamboo; in Chapter 4, the most recent and convincing tests in connections are presented; Chapter 5 firstly introduces the existing bamboo standards, then introduces the species and the structure, following with the calculation of actions and combinations, as well as the resistances, ending with the stress comparison and some modifications of the structure; in the same chapter, the dynamic analysis is performed. Chapter 6 presents the conclusions and future lines of development suggested by this work.

2. Bamboo- A Functionally Graded Material

2.1. Bamboo as a plant

The progress of structural engineering has been paralleled with the knowledge and understanding of the materials used in construction. The constitution and properties of bamboo will dictate the type of material behaviour that will occur when subjected to different stresses. To better understand this behaviour, this section introduces a description of the constitution, botany, and morphology of bamboo, as well as the topics found most relevant inherent to the bamboo plant that will impact structural behaviour.

2.1.1. Exterior Constitution

Bamboo integrates the following physical elements: branches, culm, leaves, rhizomes, sheath, and roots (Banik, 2015). The culm is the visible part of the plant, and it is hollow (though there are exceptions), tapered and segmented. It develops from shoots with its final diameter as an elongated cylindrical stem that tapers in height (eg. Kaminski et al., 2016; Titilayo Akinlabi et al., 2017; D. J. Trujillo & López, 2019). The culm anatomy combines nodes and internodes (Figure 1). The nodes consist of intermittent joints that manifest as a diaphragm to the interior of the culm, providing transverse interconnection of the culm walls. Their radially oriented cells help prevent buckling of the walls (Kaminski, Laurence, et al., 2016), assist straightening the culm and enable the conduct of water (Z. P. Shao et al., 2010). The culm sheath and branches emerge from the external part of the nodes (e.g. D. J. Trujillo & López, 2019).

The internodes are essentially hollow tubes with longitudinal oriented cells and have a varying wall thickness. The internode length is a function of the species, genetics (eg. Titilayo Akinlabi et al., 2017), habitat conditions and age (Banik, 2015), resulting in over 1000 species (Kaminski, Laurence, et al., 2016). The cross section is not perfectly circumferential, as the fibers position themselves where they are most needed throughout their life (Nogata & Takahashi, 1995).

Titilayo Akinlabi et al. (2017) and Banik (2015) show a more detailed view on the morphology of the bamboo plant. In their work, rhizomes (Figure 1) are defined as “buds which develop into shoots that emerge from the ground to form a clump of culms”.

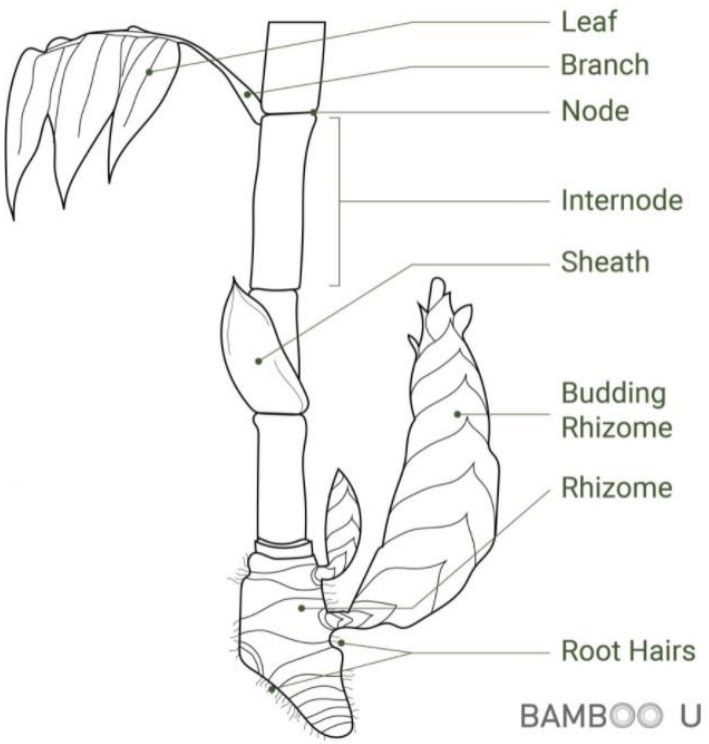

Figure 1 - Sketch of the constitutional elements of bamboo (picture from *Bamboo U*, 2021).

2.1.2. Interior Constitution

The bamboo inner culm wall is constituted by strong dark vascular bundles (vessels supported by fibers) that run parallel through the length of the culm, connected transversely by a weaker matrix called parenchyma (Liese, 1998; Dixon et al., 2015; D. J. Trujillo & López, 2019; Correal, 2019)- Figure 2. Liese (1985) found the following cell percentages: 50% parenchyma, 40% fibers and 10% conducting tissue.

The outside layer is composed of a hard and shiny skin called epidermis. Regarding the overall chemical constitution, Amada et al. (1996) found 45% cellulose, 21% lignin, 32% soluble matter, 2% ash and less than 1% nitrogen.

The vascular bundles are composed of vessels, phloem and fibers (W Liese, 1998). As a fiber reinforced composite, the vascular bundles are mainly responsible for the strength of the culm and for the transportation of water and nutrients (Dixon et al., 2015; Titilayo Akinlabi et al., 2017; D. J. Trujillo & López, 2019). More specifically, the phloem vessel transports sugars and nutrients, xylem and metaxylem vessels transport water and the sclerenchyma fibers are the principal supporting tissues within the vascular bundles of bamboo (Lo et al., 2004; Figure 3).

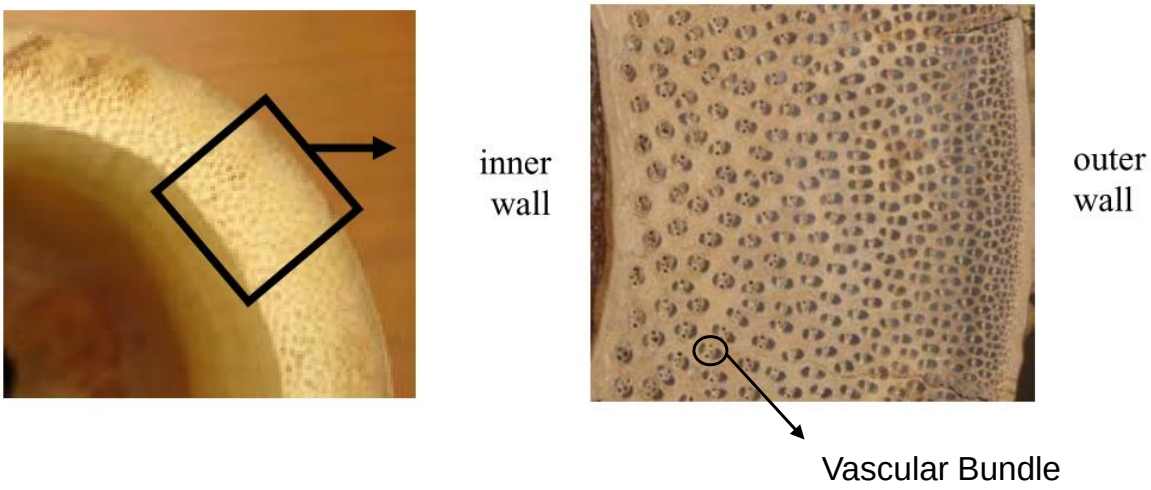

Figure 2 - Cross section of a bamboo culm- functional gradation of vascular bundles from inner to outer culm wall (adapted from Richard, 2013).

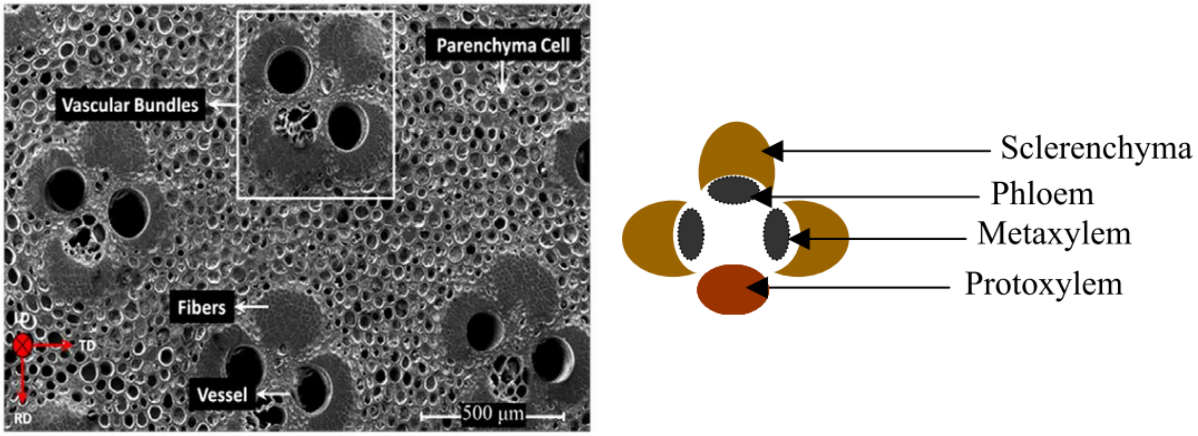

(a) (b)

Figure 3 - (a) microstructure of bamboo culm (Habibi et al., 2015); (b) constitution of a vascular bundle (Lo et al., 2004)

Bamboo is considered a functionally graded material due to the ability to adjust its constitutional properties to respond to the stresses imposed by nature during its life course. The loading it absorbs resides in the effects of its own self-weight and the lateral effects of the wind. This natural efficiency of bamboo translates in, for example, the higher concentration of vascular bundles towards the exterior of the culm wall (Figure 2). This results in a quantity of fibers roughly six times higher on the outside of the culm, making it denser, stronger and stiffer against bending (Janssen, 2000). Richard & Harries (2015) and Habibi et al. (2015) demonstrate through their studies a significant variation in mechanical properties along the culm wall. This increase of the fibers through the culm wall is comparable in purpose to the reinforcement of steel in concrete.

Moreover, the wall thickness and diameter decreases as the culm tapers in height. To oppose the loss in strength and stiffness, the vessels and amount of parenchyma diminish along the longitudinal axes and are replaced with cellulosic fibers (eg. Titilayo Akinlabi et al., 2017; Harries et al., 2017), resulting in relatively uniform engineering properties throughout its length (Amada et al., 1996).

The so-called volume fraction is defined as the ratio between fiber content and volume. Among others, Lorenzo et al. (2020) studies its variation between species, Dixon & Gibson (2014) demonstrate its radial increase through the culm wall and Godina & Lorenzo (2015) its increase in height.

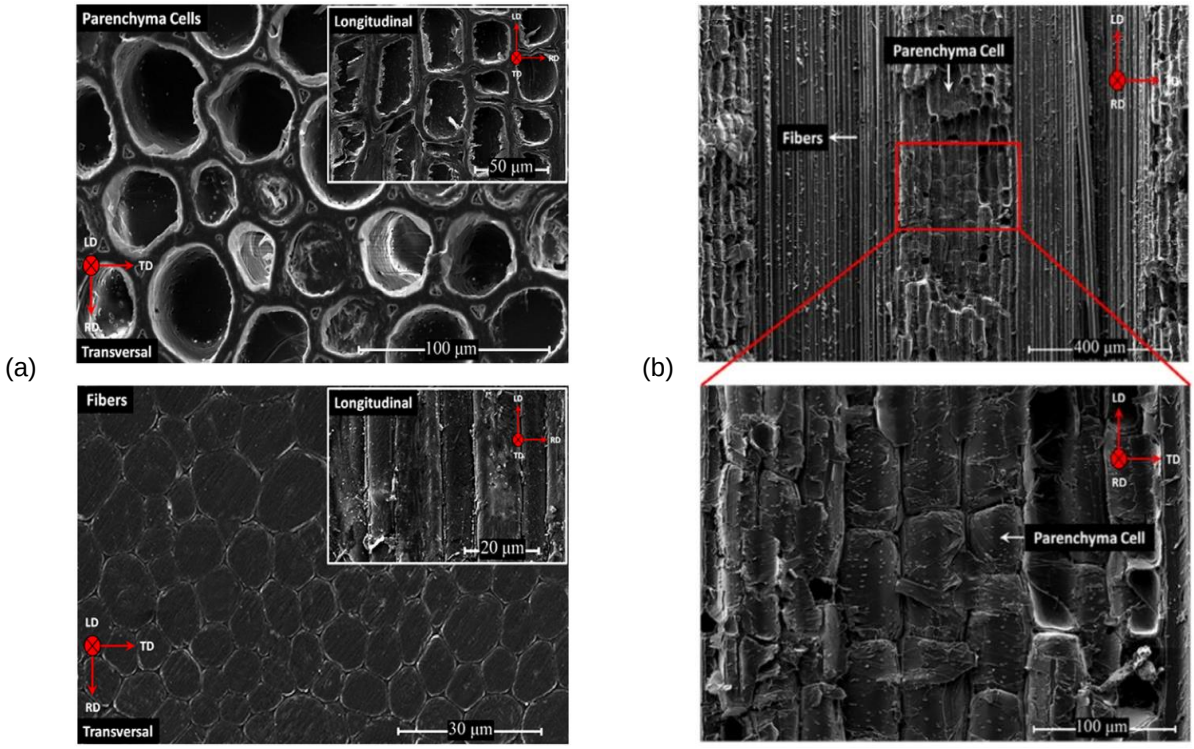

Figure 4 - (a) microstructure of parenchyma cells and bamboo fibers in transversal and longitudinal direction; (b) magnification view of the wall structure of the intact parenchyma cells (Habibi et al., 2015).

2.2. Material Properties of Bamboo

2.2.1. Effect of Age

Bamboo can grow exceptionally fast, up to more than 1 meter a day (Titilayo Akinlabi et al., 2017; Rabik & Brown, 2004). However, it requires a maturation period to enhance the physical and mechanical properties of bamboo. On the other hand, the properties of bamboo will decay after they reach their peak if the culms are not harvested (Zhou (1981); Lu et al. (1985)- Figure 5, Figure 6). Therefore, the bamboo age at harvest will largely impact its structural applicability. D. J. Trujillo & López (2019) affirm the maturing period ranges from 3 to 6 years, although in their work cite (Liese, 1985) stating it is a general assumption that bamboo matures after 3 years. Correal D. & Arbeláez C. (2010) concluded

through testing that mature age is reached between 3 and 4 years of age, analogously to the years where the density and strength peaked. In this study, 5 year old culms showed lower values of density and strength. Trujillo et al. (2017) found a continuous increase of density with age, yet a peak of strength in culms between 4 and 5 years. Likewise, Kaminski et al. (2016) states that to mature to full strength, culms take 3 to 5 years, and that after 5 to 6 years the culm strength begins deteriorating.

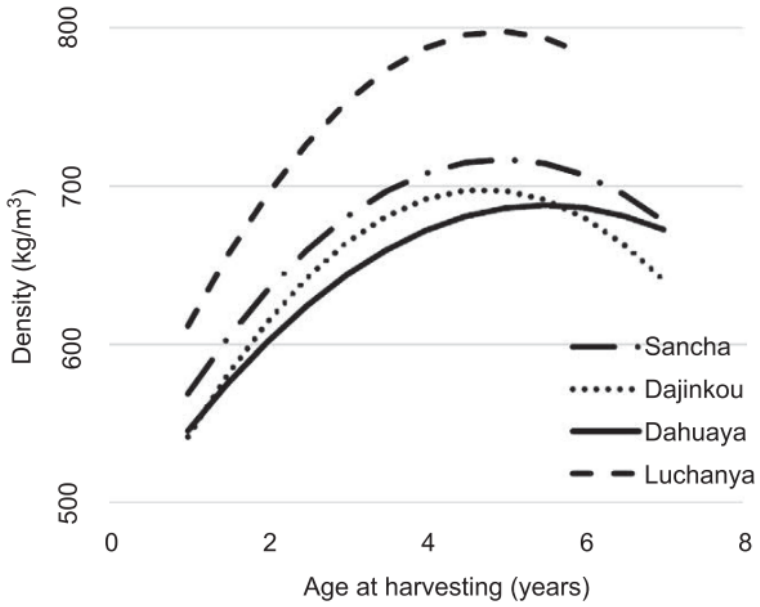

Figure 5 - Effect of age at harvesting on density for Phyllostachys glauca bamboo from four different regions of Shandong province, China (Lu et al. (1985)).

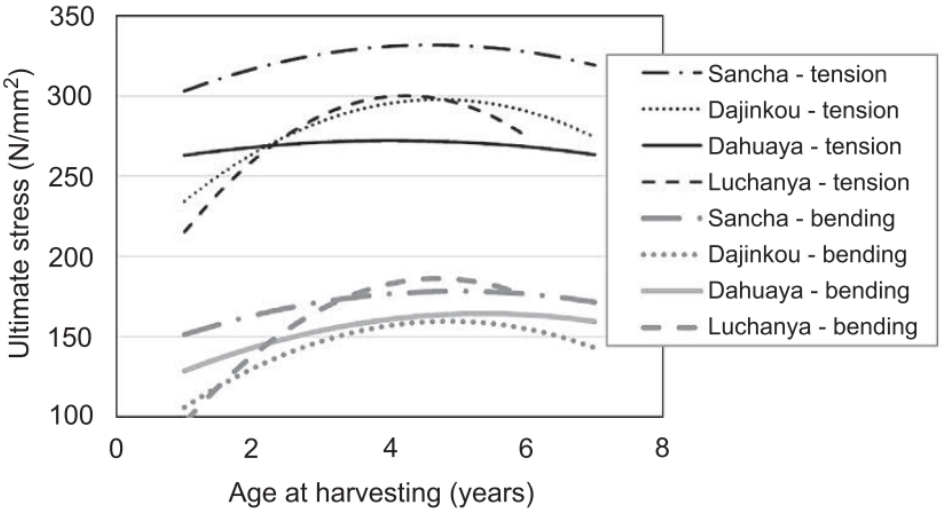

Figure 6 - Effect of age at harvesting on strength for Phyllostachys glauca from four different regions of Shandong province, China (Lu et al. (1985)).

As for the reason why the properties of bamboo are enhanced with age, it relates to the hardening of the parenchyma tissue matrix which lignifies the culm, resulting in the increase of the culm's density,

stiffness and strength (Liese, 1998; Kaminski et al, 2016; Harries et al, 2017). Berndsen (2008) references Chun Z. (2003) demonstrating visually the decrease of the vessels' diameter and the increase in density throughout the years (Figure 7).

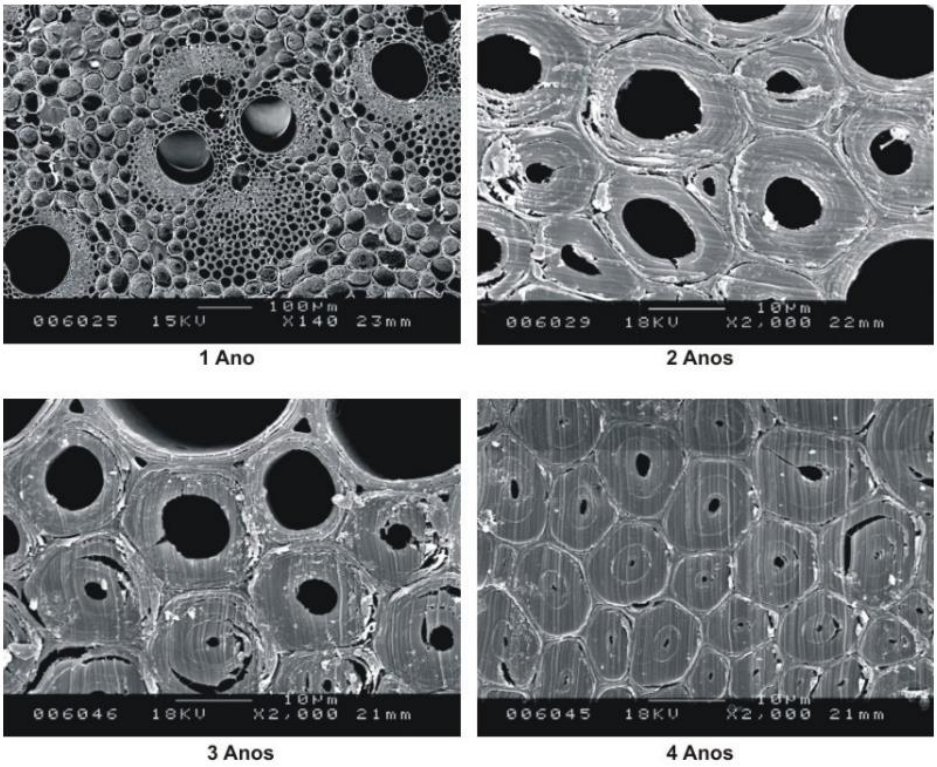

Figure 7 - Increase of density through age (Chun, 2003- ref. by Berndsen, 2008)

According to Li et al. (2007), bamboo presents a lignin content around 20 to 26%, similar to that of soft (24-37%) and hard (17-30%) wood species.

Besides density and strength, moisture content at harvest (Figure 8) and modulus of elasticity also have been observed to be affected by the age of the culm at harvesting. Regarding the modulus of elasticity (MOE), Harries and Sharma (2020) found conflicting conclusions in the existing literature. Trujillo et al. (2017) concluded MOE peaked around 3-4 years of age, while Correal D. & Arbeláez C. (2010) found no significant relation between specimen age and MOE in his work.

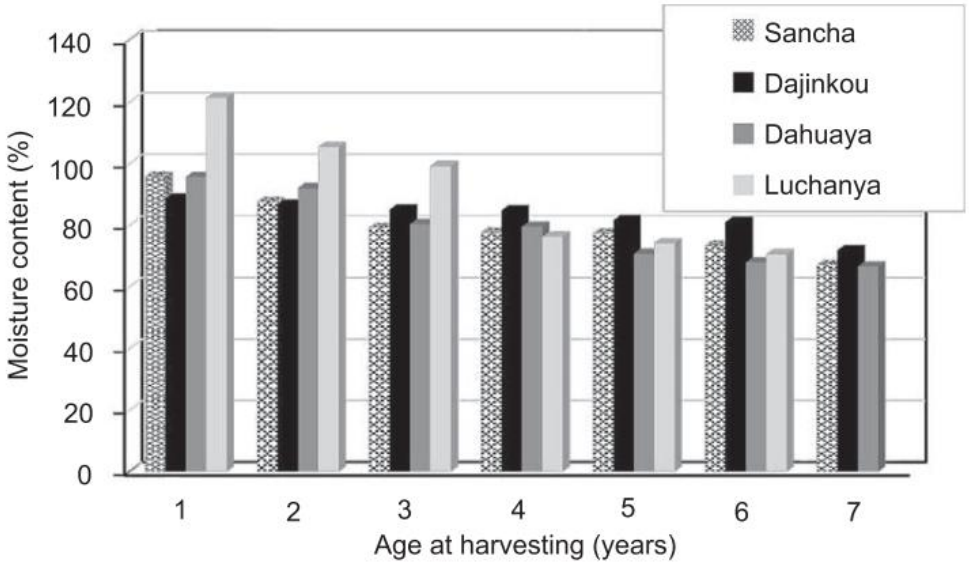

Figure 8 - Effect of age at harvesting on moisture content for Phyllostachys glauca from four different regions of Shangdong province, (Lu et al.,1985).

The studies quoted in this section lead to the conclusion that the optimal time to harvest bamboo for structural applications is around the 4 year mark, although after 3 years bamboo is very likely to have matured.

2.2.2. Effect of Density

The density of bamboo depends on fiber content, fiber diameter, and cell wall thickness (Janssen, 2000). The density of most bamboo is 600 – 800 kg/m^3 but will vary with species, growing circumstances, and height (Harries et al., 2017). Kaminski et al. (2016) argue the dry density of bamboo is typically about 500-800 kg/m^3. Nevertheless, it is important to register the bamboo density before use according to the recommendations of the international standards.

In a similar manner to timber and other materials, density correlates to the strength of bamboo. This correlation has been observed to be linear by Ota (1950), Sekhar et al. (1962) and Zhou (1981). More recently, Lo et al. (2004) also concluded how density is a good indicator of strength capacity of bamboo, while Trujillo et al. (2017) shows the same evidence, yet with a less linear distribution (Figure 9).

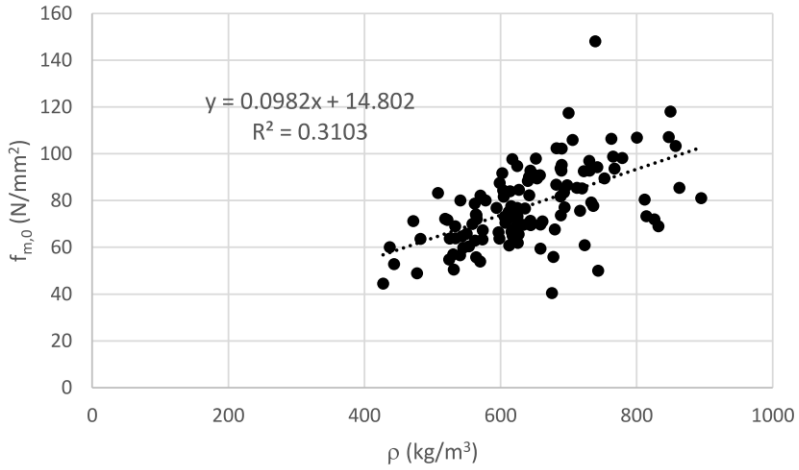

Figure 9 - Relation between density and bending strength from Guadua angustifolia Kunth (Guadua a.k.) found in (D. Trujillo et al., 2017).

As mentioned, density increases radially, with age and in height. The latest is demonstrated in Figure 10 by the work of Zhou (1981).

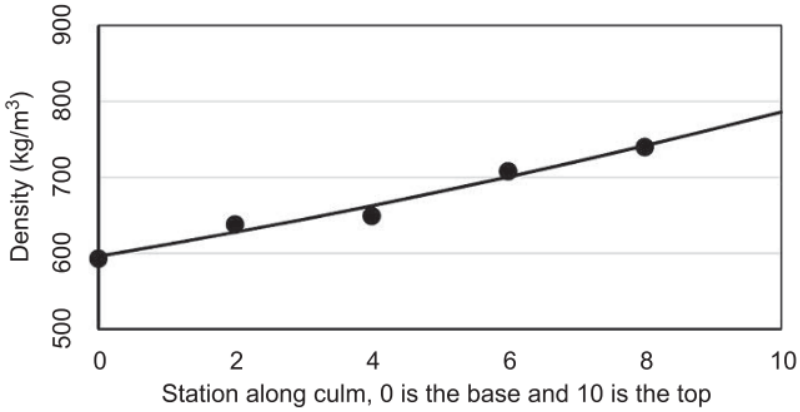

Figure 10 - Variation of density along the height of the culm (Zhou, 1981).

2.2.3. Effect of Moisture Content

The effect of moisture content (MC) of bamboo is broadly considered crucial when analysing the properties and strength of bamboo, as it affects both short and long-term performance. In a similar manner to timber, green bamboo (freshly harvested) has lower strength than dry bamboo. Green bamboo has a moisture content higher than the fiber saturation point (FSP), which ranges between 20% to 30% (F. Correal, 2019). Above the FSP, free water accumulates in the cell cavity (Hallwood and Horrobin, 1946). Bamboo with a moisture content close to the equilibrium moisture content (MC after a long period of time in a given environment) can be considered dry bamboo, with values ranging between about 10% to 18% (D. Trujillo & Jangra, 2016).

Jiang et al. (2012) states it is well known that for wood, a decrease in MC below the FSP has significant influence in the mechanical properties, as for MC values above the saturation-point, specimens show stable strengths. D. J. Trujillo & López (2019) state the same occurs for bamboo, showing test results demonstrating inverse proportionality between MC and strength for lower values of MC (Figure 11). This trend can also be noticed in the test results of Sánchez Cruz & Morales (2019) and Jiang et al. (2012), who likewise investigated the variation of the mechanical properties with MC.

After Limaye (1952), in a significant amount of literature regarding mechanical properties of bamboo, results for both green and dry bamboo are displayed, having dry bamboo the edge in the results, repeatedly. The international standard for testing (ISO 22157:2019) requires testing bamboo at a dry condition ((12 ± 3) % moisture content), since it is more representative of service conditions. In addition, the structural design standard ISO 22156:2021 (addressed in 5.1) sorts 3 different service classes to consider the correct environment of the bamboo *in situ*.

As for the variation through culm length, MC decreases from the bottom to the top, contrarily to density (e.g. Zhou (1981); Abdul Latif et al. (1990); Titilayo Akinlabi et al. (2017)), independently of the time of harvesting (Wakchaure & Kute, 2012). Anokye et al. (2014) conclude the same trend, although stating the difference was not statistically significant.

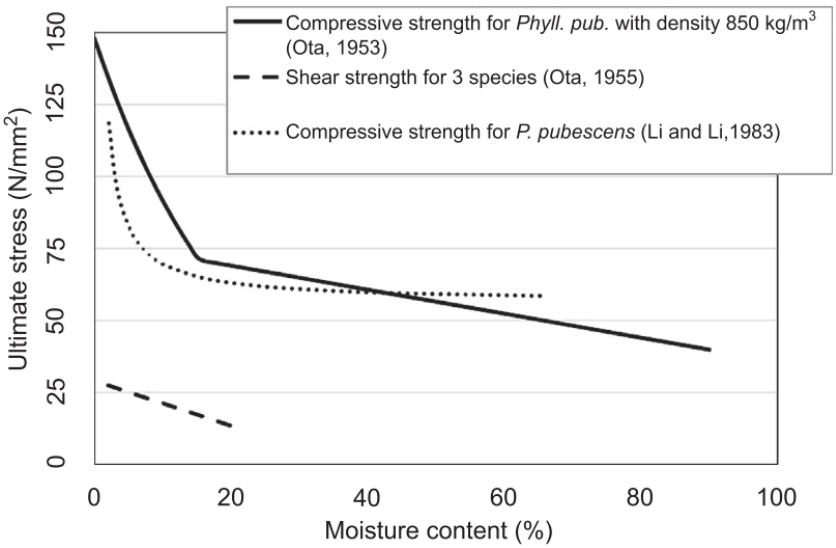

Figure 11 - Effect of moisture content in ultimate stresses (D. J. Trujillo & López, 2019).

As seen, bamboo does not present uniform properties. Nevertheless, the variations are not particularly substantial and therefore do not compromise the structural use of bamboo. It just evidences the significance in registering all of these relevant characteristics to properly grade the culms, enabling the safe use of this natural element.

3. Durability and Treatments

The evolution of bamboo treatments is one of the most consequential reasons why bamboo is now leaning towards becoming a conventional material. The common consideration that bamboo is a poor man's timber came about due to its lack of durability. This chapter summarises the current state of bamboo treatment options, methods, and the importance of seasoning and durability by design.

3.1. Causes of decay

It is common understanding in the referenced literature that if untreated, bamboo will not last. It is a vulnerable material, and can deteriorate in as little as less than half a year (e.g Kaminski, 2018). Bamboo's lack of natural toxins, high levels of starch and thin walls make it more susceptible to decay than timber (Kaminski et al., 2020).

Despite there being an immense diversity in pests and diseases that can damage bamboo (described in Shu & Wang, 2015), the three main causes of decay are beetles, termites and fungal attack (rot) (e.g Kaminski et al. 2016). These attacks emerge immediately after harvesting, depreciating the properties and applicability of bamboo (Titilayo Akinlabi et al. (2017)).

3.1.1. Beetles

Beetles are attracted to the starch in bamboo. For this reason, the rate of attack is faster with fresh green bamboo, as its starch content is higher. Nevertheless, dry bamboo can also be easily attacked (Liese et al., 2002). The beetles lay eggs inside the culm, and after the larvae eat along the culm without being noticed, it escapes leaving small round exit holes from 1 to 6 mm (Kaminski et al. (2016); Figure 12). Since they also feed from the soluble carbohydrates in the parenchyma cells (more present towards the inner part of the culm), it can lead to a misevaluation of the damage (Liese & Tang, 2015).

Figure 12- Beetle exit holes visible inside of bamboo (Kaminski, 2018).

3.1.2. Termites

Termites are also attracted to starch but have enzymes that allow them to disintegrate the cellulose present in the culms. The subterranean termites are translucent so often build tunnels to avoid sunlight. As they live in large colonies, they can cause great damage rapidly (Kaminski, 2018b; Figure 13). Dry-wood termites enter the bamboo through fissures or openings, and therefore can attack structures above ground level (Walter Liese & Tang, 2015).

Figure 13- Significant termite damage to bamboo column in Costa Rica (Kaminski, 2018).

3.1.3. Rot

Rot is generated by a fungus that needs to remain with at least about 20% of moisture content to survive, suggesting that bamboo will only rot if exposed to rain or ground moisture (Kaminski et al, 2016). It is also not immediately noticeable since it is more likely to occur in hidden, unventilated areas.
This cause of decay is the hardest to resist, and the best way to do it is by using durability by design, a concept approached ahead (chapter 3.5).

Figure 14- Boron treated bamboo exposed to rain and sun for approximately 10 years showing signs of fungal damage, splitting and bleaching (Kaminski et al., 2016).

3.2. Preservative Treatment Options

Preservatives are toxins that when added to bamboo, make it more resistant to the attacks discussed. When deciding what treatment option or method to apply, it is important to consider factors like the quantity of bamboo to be treated, the toxicity of the chemical through the application, use and disposal, its availability, the intended use of the bamboo, among others (Kaminski et al. (2016)).

There are traditional non-chemical techniques such as Curing, Waterlogging and Smoking, as well as chemical methods such as the Butt Treatment, Old Engine Oil and more (e.g Titilayo Akinlabi et al. (2017)). These methods will not be discussed due to their limited effectiveness or high level of toxicity.

Any treatments using Arsenic, as some older copper-based preservatives, are now highly unrecommended as they cause major health and safety risks, and have been banned from most countries (Kaminski et al., 2020). Painting with conventional paint is also unadvised, since although it reduces the water absorbed from the rain, water will eventually infiltrate due to splits or deterioration of the paint and get trapped on the inside, making it more favourable to rot (Kaminski, 2018).

As a result, from the numerous types of treatment currently available, two are widely considered by far the most appropriate. They are Boron and modern copper-based wood preservatives, being Boron the most appropriate overall.

3.2.1. Boron

This chemical element is the most popular and appropriate by virtue of its efficiency, cost, low toxicity and easy applicability. Furthermore, it proves to be competent (Kaminski, 2013).

It has both insecticidal and fungicidal properties, yet boron treated bamboo (or treated with any of the boron- containing compounds) cannot be exposed to rain since the preservative will eventually dissolve (Kaminski, 2018). Liese & Tang (2015) also declare it to be ineffective against soft rot.

It is typically used in compound form, as a salt and dissolves easily in water (Hodgkin, 2009). The most regularly used form is disodium octaborate tetrahydrate (Tim-bor, Solubor or DOT), that “presents little or no hazard (to humans) and has low acute oral and even lower dermal toxicity” (InCide Technologies, 2013). Essentially, if not in contact in high concentrations, it is harmless or safe to use (e.g Correal, 2019; Hodgkin, 2009) and available in most countries for a relatively cheap price. It simply needs to be added water and the solution can be reused multiple times (Kaminski et al. (2016)).

Borax and boric acid are other equally effective boron containing compounds. They have to be used together as they are only soluble when mixed (Kaminski, 2018). Methods to apply this solution can be found in 3.3.

3.2.2. Modern copper-based preservatives

These preservatives no longer have arsenic and chromium, and therefore are no longer as toxic as previous forms. Unlike boron, they are chemically relatively well-fixed into the bamboo, meaning it can more easily be utilised externally or in contact with the ground Kaminski et al. (2016). For the same reason, it is safe to use. However, it can’t be burnt end-of-life as it may release hazardous chemicals (Kaminski et al., 2020). Although it is quite effective, applying this preservative comes out quite

expensive, as not only it implies semi-industrial pressure treatments (3.3.4), but also because the bamboo must be kiln-dried beforehand (Kaminski et al., 2016).

Gauss et al. (2020) investigated the effect on the mechanical properties and treatability of *Phyllostachys edulis* (Moso bamboo), as it is the most widely commercialized bamboo species. In this investigation, treatments with disodium octaborate tetrahydrate (DOT) and chromated copper borate (CCB) were performed. Five mechanical property tests were not affected by treatment procedures, and no difference between CCB and DOT was found.

3.3. Treatment methods

Contrarily to timber, bamboo does not have ray cells that provide a radial transportation system through the wall thickness (Correal, 2019; Liese & Tang, 2015). Thus, the penetration of chemicals into bamboo is not as easy. From the several existent treatment methods, the most common to treat full culm bamboo are described under, the first three applicable using boron.

3.3.1. Soaking

This method is extremely simple, cheap, and effective. The bamboo culms are immersed in a bath of the chemical for several days (different authors state between 7 to 14 days), for the slow penetration to occur (Figure 15). Before placing the culms inside, it is good practice to puncture through all the nodal diaphragms, to ensure that the chemical spreads properly (Correal, 2019; Kaminski et al. (2016)). The bath liquid can be reused several times.

After harvesting, the cell walls of the bamboo start to close, therefore it is recommended to initiate this procedure within the first 7-14 days. Essentially, as soon as possible, so that boron can diffuse through and not compromise the effectiveness of the treatment (Kaminski, 2018).

Figure 15- Bath/Soaking method using boron, Colombia (Kaminski et al., 2016)

3.3.2. Vertical soak diffusion

The Vertical Soak Diffusion method consists in pouring the chemicals in an upright positioned culm from the top (figure). The diaphragms must also be punctured through all the length but the last couple of nodes. This way, the chemicals will not exit from the bottom but instead slowly diffuse from the inside outward. A dye may be added to allow visual confirmation that the chemical has been spread correctly (Kaminski et al. (2016)).

As the previous method, vertical soak diffusion also requires that treatment is done quickly after harvesting, preventing cells from closing.

3.3.3. Modified Boucherie Method

The Modified Boucherie is a method in which the preservative is pressured with an air pump making the liquid chemical pass through the culm vessels until it reaches the other end of the culm (Janssen, 2000). Because it uses pressure, it can take as little as 30 min per culm. It is very effective as well, but it will not be if the bamboo is treated more than 12 hours after being harvested (Kaminski et al. (2016)). Same authors note that this is the only method that avoids the rupture of the nodal diaphragms. This can help control buckling of the culm, splitting, and improve the reliability in the process of filling the internode when building structural connections (chapter 4 on connections). The technology involved and requirement of the freshness of the culms are the inconveniences of this method.

3.3.4. Pressure Treatment

This method is between the best to preserve bamboo, yet it is quite expensive. This is because it needs specialized equipment to apply the pressure (F. Correal, 2019). As a reference, the equipment involves a 6m long cylinder and estimated cost for treatment is US$ 5000 including transportation and installation charges (INBAR, 2020). It is therefore more appropriate for large scale treatments. It has the advantages of minimizing the risk of chemical spills and it is able to provide uniform quality treated material.

3.4. Seasoning/Drying

Seasoning of bamboo consists in drying the culms in order to lower the moisture content closer to the equilibrium moisture content in service (e.g Kaminski et al. (2016)). This is extremely relevant since not only is bamboo stronger and less susceptible to decay when dry, but also because shrinkage is directly correlated to moisture content (Liese & Tang, 2015).

Splitting tends to occur while seasoning. Cracks and splits will affect the capacity of the culm (although the extent of it is still unestablished), so it is recommended to control the process and grade bamboo only after the drying process (D. Trujillo & Jangra, 2016). Shrinking in service conditions would generate dimensional changes that could also affect connections (Liese & Tang, 2015; Kaminski et al., 2016). Thus, it is better to work with dry bamboo.

The seasoning process is then ideally done slowly, so that the bamboo shrinks uniformly, and cracks and splits don’t occur. Given the hollow section, it is a significantly slow process, so solar (air) or heated kilns are used to make it faster (Titilayo Akinlabi et al., 2017).

3.4.1. Air drying

Air drying bamboo within a well-ventilated environment or in the sun light is the most economical out of the two known seasoning techniques. The downside is the time it takes until the desired moisture content is reached. It can take from weeks up to months, which increases exposure to fungus (Titilayo Akinlabi et al., 2017). The weather conditions affect air-drying greatly, and since they cannot be regulated, it's not possible to monitor the drying process (Liese & Tang, 2015).

Figure 16- Seasoning of bamboo in Colombia (Kaminski et al., 2016).

3.4.2. Kiln-Drying

Kiln-Drying is a shorter and more efficient process, which injects heat into chambers where the bamboo culms are stacked (Titilayo Akinlabi et al., 2017). With suitable conditions of temperature, relative humidity and air circulation, kiln drying boron treated bamboo culms have proved to be applied successfully, forming less splits than untreated culms (Tang et al., 2013). More recommended for large numbers and better guarantees the quality of the seasoning process.

3.5. Durability by design

This concept means designing a structure with characteristics that improve its durability. Kaminski et al. (2020) states this is the single most important way to preserve the durability of a bamboo structure, arguing it might even be more relevant than the durability treatments. This is because no treatment allows bamboo to really last without preventing it from rotting, therefore bamboo needs to be fully protected from the rain. The following measures are examples of how to implement durability by design ((Kaminski, 2018); (Titilayo Akinlabi et al., 2017); (Hodgkin, 2009); (Kaminski et al., 2020); (Kaminski et al. 2016)):

- Elevate and separate the bamboo frame from the ground;
- Create a watertight impermeable roof and walls to protect the bamboo frames;
- Create an overhang on all sides to protect the bamboo from driving rain, considering the additional wind loads;
- Allow proper ventilation inside the structure;

- Avoid water traps, especially at bases of the culms, horizontal beams and connections;
- Elevate the structure, avoiding ground contact and with areas where water can access;
- Do not cast bamboo into concrete: it attracts and traps water from the upper parts of the culm or from the water in the concrete, as well as creating a way for termites after concrete cracks from temperature variations or shrinkage;
- Ensure adequate drainage;
- Remove termite shelter tubes;

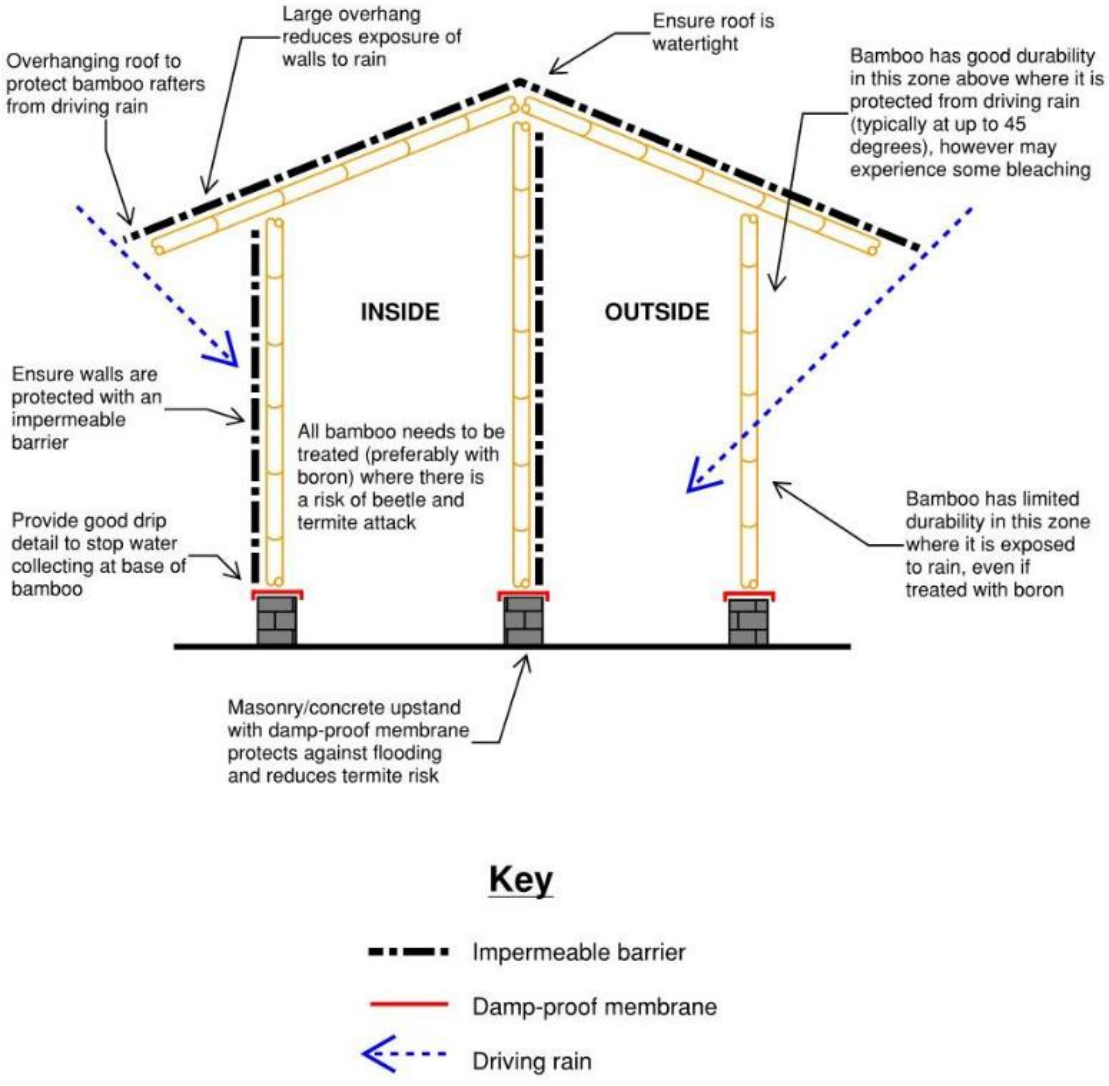

Figure 17- Recommendations for detailing bamboo structures to protect against rot and insects (Kaminski et al., 2016).

3.6. Summary

Bamboo is a vulnerable material that without treatments can deteriorate quickly due to beetles, termites and fungus. To treat it, Boron is the simplest, most economical, effective and sustainable option amongst

other treatment possibilities. However, it is vital to protect it from rain, as otherwise the chemical will wash out and the bamboo will rot. For this reason, durability by design is indispensable.

Although less recent literature predicted that the lifespan of bamboo treated with boron without water exposure would be about 30+ years, authors in recent works as Kaminski et al. (2020) argue it can last a lifetime (50+ years). This of course if all cautious steps are taken:

- Selecting mature bamboo;
- Harvesting at appropriate times (when starch and MC levels are lower);
- Seasoning;
- Modern methods of preservation;
- Durability by design;

4. Connections

Connections are crucial for the integrity and safety of any structure. The joints in bamboo are particularly challenging due to its round, hollow, tapered, and thin-walled constitution. This makes it hard to find reliable connections in the construction process, more than in other materials such as timber (Correal, 2019; Hong et al., 2019).

Besides its dimensional characteristics, bamboo's dominant tendency to split (Mitch et al., 2010) and low allowable shear stress make connections regarded as the weakest parts in bamboo constructions (e.g Awaludin & Andriani, 2014).

Bamboo structural members are also more efficient in axial loading due to the difficulty to provide moment-resisting connections in bamboo. Thus, no moment transmission between connected culms should be considered (only pin-connected), unless for continuous elements (Correal, 2019; Kaminski, Laurence, & Trujillo, 2016).

This chapter presents a review of the most successful studies found for connections in bamboo, sorted by the elements of their constitution.

4.1. Types of Connections

4.1.1. Bolted Connections

Bolts are the most broadly adopted connectors for their simplicity, efficiency and cost (Hong et al., 2019). Sassu et al. (2016) proposed three joints for planar truss structures, focussing on low-cost dowelled and bolted connections using plates. Low technology, simple repair and satisfactory structural performances were achieved. In other studies (e.g Paraskeva et al., 2019), simply bolted connections (with no other connecting elements) displayed brittle splitting behaviour and poor mechanical performance. Therefore, their use alone was discouraged by the authors.

4.1.2. Steel Member Connections

There are many ways to connect bamboo through steel members, from simpler ways to more complex prefabricated solutions that try to meet the mechanical and architectural requirements. Although prefabricated solutions are accurate, durable, and have all the advantages inherent to steel, the fabrication process is expensive and most likely not universal, which makes it difficult to connect with such a variable material as bamboo (Hong et al., 2019).

Fu et al. (2013) developed comparative loading tests of different joint methods, all including a metal sleeve. The four connections created (named and illustrated in Figure 18) were submitted to static tensile, compressive, and bending tests. Results between specimens were compared, and significant values of strength and ductility were found. The weight and cost of the solutions were not mentioned, although these are likely to be setbacks. Relative position over time of any piped steel solutions is also questioned by Hong et al. (2019).

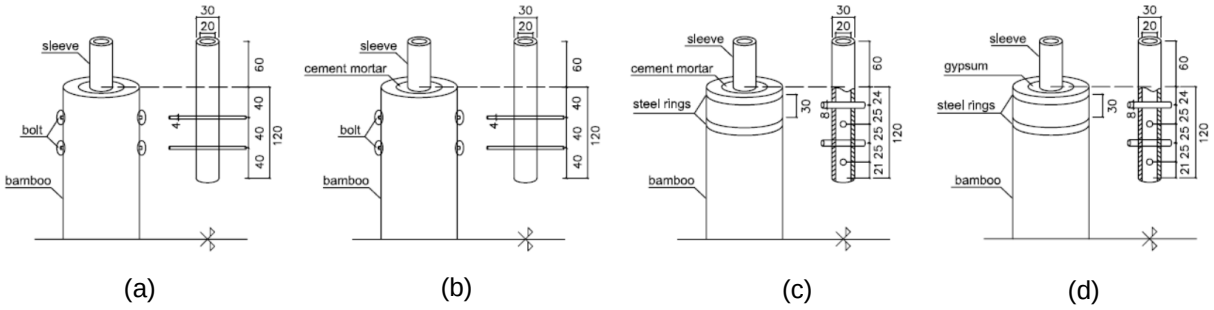

Figure 18- Joints and dimensions developed in (Fu et al., 2013): (a) sleeve-bolt (b) sleeve-bolt-cement (c) sleeve-cement d) sleeve-gypsum

Paraskeva et al. (2019) studied the behaviour of three connections: bolted (Type A), bolted enhanced with hose-clamps (Type B), and bolted reinforced with hose-clamps and infill mortar (Type C)- Figure 19. For the latest, the mortar filling average mix ratio took 2.5 parts cement, 1 part sand, and 1.2 parts water by mass. Compressive, tensile, and bending tests were developed.

Plain bolted connections (Type A) were discouraged due to the quick brittle splitting behaviour, as noted previously. The hose-clamps proved to prevent splitting drastically, confining the bamboo and improving strength and ductility. They effectively resist the brittle splitting behaviour, which is extremely valuable as that is the main failure mode. As for Type C, the mortar infill improves the axial performance and resistance to crushing, yet the infill reduces the ductility since it restrains the bolt deformation. The hose-clamps prove to be the most significant contribution to ductility.

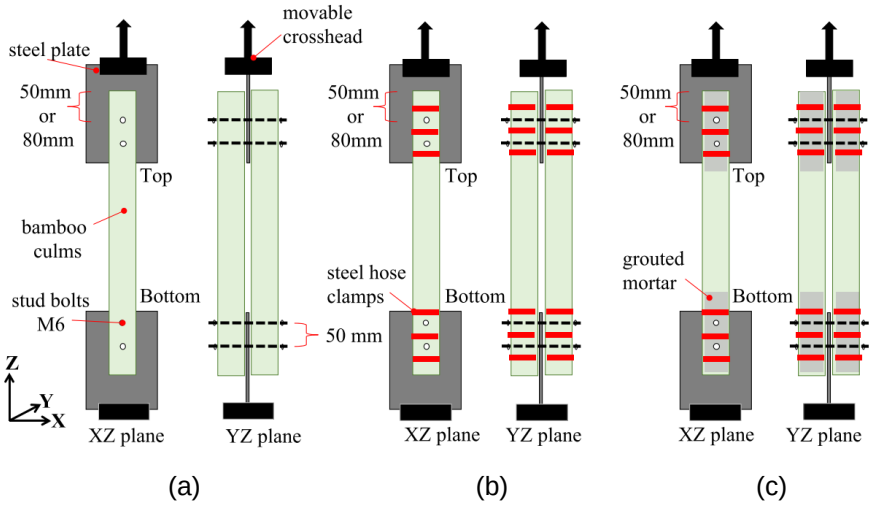

Figure 19- Specimens from proposal by Paraskeva et al. (2019): (a) Type A, (b) Type B, and (c) Type C.

The study relevantly proves that the European Yield Model (L.A. Soltis, 1991) which refers to dowelled timber connections can predict analytically the yield load achieved experimentally with satisfying accuracy, verifying that bamboo to steel connections can be reliable. Authors note that besides positive

results, there is room for improvements as the connections are still short in axial strength compared to the bamboo culm.

Moran & Silva, 2017 created a connection with the purpose of transmitting moment, so that it can be possible to exclude diagonal elements in some applications. This beam-column connection (Figure 20) uses five pairs of thin and light semi-rings that can adjust to variable sizes, solving the problem of dissimilarity. Results of strength and ductility significantly overcame values from previous studies. Once again, the semi-rings prove to increase ductility and avoid typical splitting failures (as had been reported by Moran & Silva, 2016), as well as providing a light weight solution. Finite element simulations of the connection also showed consistent and favourable results.

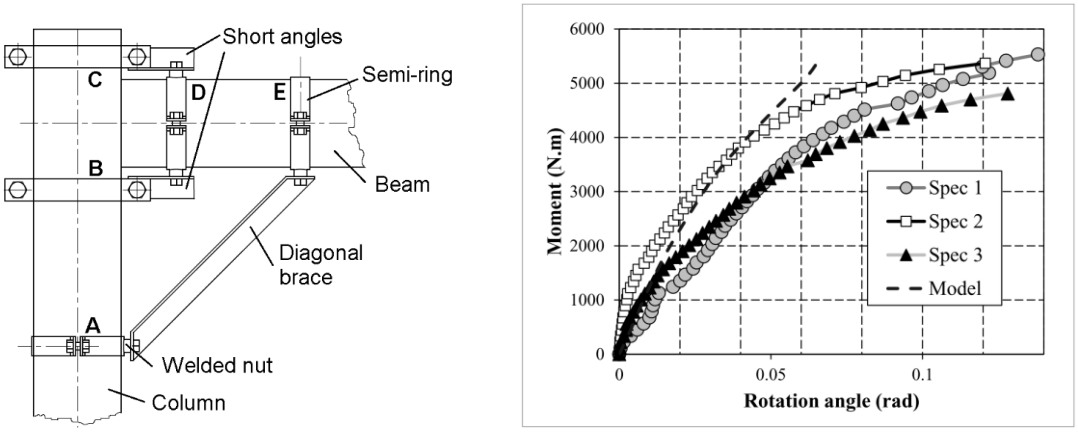

(a) (b)

Figure 20- (a) Beam-column connection studied in (Moran & Silva, 2017); (b) Curves of moment versus angle of rotation of the connection

4.1.3. Infilled Bamboo Connections

Infilled bamboo connections have become a very popular solution. Cement mortar is the most common filling material, as it is economical and easy to obtain (F. Correal, 2019). Same author mentions Colombian standard NSR-10 for its recommendation of a minimum of cement:sand ratio of 1:3, as well as using a plasticizer additive to establish wanted fluidity.

Opening bolt holes weakens bamboo components and enhances the probability of splitting. To overcome this tendency, placing infills through the cavity of the bolts, ensured the stiffness and stability of the joints (Hong et al., 2019). Mortar injected joints show very significant improvements in the compressive strength and bearing capacity of joints (e.g J. F. Correal & Echeverry, 2015). Moreover, it is recommended to use mortar infill whenever transverse crushing loads are applied, as it improves resistance and helps fixing dowel-type connections (F. Correal, 2019; Widyowijatnoko & Harries, 2019). Nevertheless, there are vulnerabilities associated with mortar filled bamboo. Several authors as Kaminski et al. (2016) state bolted connections with mortar are relatively brittle, therefore remind to use good seismic design principles and more locally ductile connections to achieve desired structural

behaviour. Awaludin & Andriani (2014) question the different shrinkage and swelling ratios between mortar and bamboo and point out the inevitable weight addition of the mortar in this solution.
Li et al. (2017) studied the axial load behaviour of Moso bamboo by filling concrete or mortar in the bamboo cavity, comparing the variations due to the presence of a node, the infill material and the horizontal stiffener or reinforcement. Once again, infilled bamboo axial load bearing capacity proved to be substantially greater than conventional bamboo. Important to note all infilled specimens failed in the mode of splitting (delayed when in the presence of either a node or a stiffener). Ductility for concrete infilled bamboo increased with steel reinforcement. A method to predict the ultimate bearing capacity was proposed in this study which demonstrated to be appropriate.
More research needs to be done to find new infill materials that provide desirable mechanical properties, are light weight, and easy to apply F. Correal, 2019. Author notes wood's specific weight is similar, yet the applicability is challenging.

4.1.4. Other Types of Connections

There are vastly different propositions to solve the problem of connections. From the many traditional ways to connect bamboo, most involve lashing. This method is adjustable and low price, and the rope avoids cutting bamboo, but it demonstrates low efficiency and insufficient stiffness. Moreover, this method depends on human operation and is affected by weather conditions (Hong et al., 2019). This solution is still applied in many modern structures due to the aesthetic aspect, most commonly when tying together many small diameter culms or bamboo splits. The latest are often used when a curvature of bamboo is intended. Another option for the rope is a metal clamp, as in Figure 21.

(a) (b)

Figure 21- Large metal clamp connection in Luum Temple, Tulum, Mexico (*Galeria de Templo Luum / CO-LAB Design Office*)

Kaminski, Lawrence, et al. (2016) remind that although traditional bamboo constructions have performed well in earthquakes in the past, modern constructions tend to be heavier and have more restricted movements. Therefore, they require more certainty of resistance to earthquakes to brittle

failure. The success from previous structures is granted not only to bamboo's lightweight and flexible nature, but also to the ductility provided by connections using nails, for example in vernacular bahareque constructions, thoroughly described by Kaminski, Lawrence, & Trujillo (2016). Trujillo & Malkowska (2018) developed equations of Eurocode 5 to assess embedment strength, withdrawal capacity and slip modulus of self-tapping screws in bamboo.

Awaludin & Andriani (2014) proposed wrapping bamboo poles in Fiber Reinforced Plastic (FRP) in the form of sheets to achieve better performance of bolted bamboo connections. Results from testing showed significant increase in lateral load capacity and joint slip modulus.

Widyowijatnoko & Harries (2019), among other proposals, show alternatives using modern pretensioned lashed connections. Authors mention Widyowijatnoko (2012) demonstrated this solution was theoretically capable of reaching the full capacity of a bamboo culm in tension.

Another successful joint proposal is the one from (Lefevre et al., 2019), which consists of wooden blocks that connect to bamboo through machined pegs and hose clamps (Figure 22). Different positions of the clamps and different types of wood were studied. The best results were achieved using hose clamps at the two ends of the peg and using hardwood. This design led to values of 88.4 MPa of maximum bending strength (value greater than in any published literature, approximately 70% of culm bending strength), and shear strength of 18.5 MPa, also a significant number.

This solution is relatively light, uses readily available and relatively cost-effective materials, and proves to have compelling mechanical properties. The obstacle is to fit the wooden pegs in the bamboo culms in the correct manner, as culms vary in dimension.

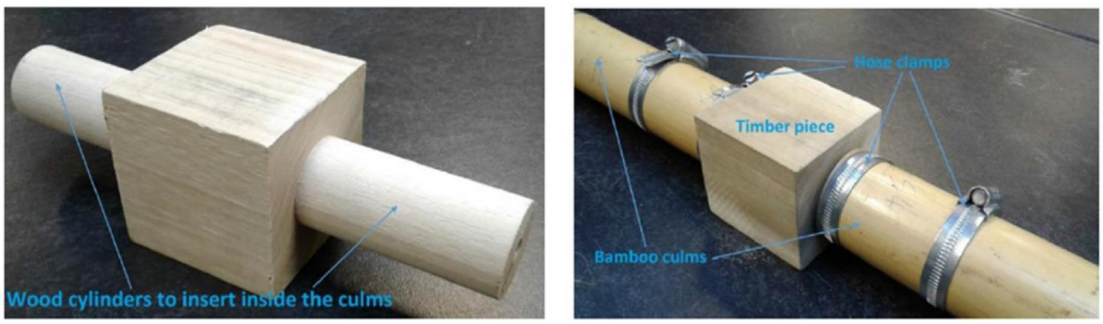

(a) (b)

Figure 22- (a) Wooden block with two pegs (b) block connected to culms by two hose clamps per joint (Lefevre et al., 2019)

4.2. Summary

Connections have not yet reached an extensive level of investigation. The peer-reviewed research on bamboo connections remains limited (Paraskeva et al., 2019). Moreover, joints are in nearly all cases the most vulnerable parts in bamboo structures (Kaminski, Lawrence, & Trujillo, 2016). The number of tests developed is still a long way in comparison with timber, and therefore it is necessary to create a

larger number of studies so that with that data, a design system for bamboo connections can be established (Hong et al., 2019).

From the variety of connections presented, radial clamping to resist splitting was notably efficient. This method is also suggested by the structural design international standard, in a chapter dedicated to joints and chapters. In it, the methods of testing, determination of joint properties and characteristic values are advised to be performed according to the respective timber standards.

The review in the present chapter indicates a variability between attributes and setbacks of each solution. Weight, strength, ductility, cost, reliability, efficiency and durability of the connection are relevant.

5. Case Study- Structural Analysis

After the previous literature review of topics inherently affiliated with bamboo structural engineering, the present chapter looks to display the steps that led to the safety verification of a bamboo structure.

Firstly, an introduction to the international standards and their relevance to the design is presented. Then follows the justification of the species chosen and the design principles used to create the structure. After, the definition of the actions according to the Eurocodes, followed by the calculation of the allowable strengths and verifications conforming to the international standard. Subsequently, the analysis of the stresses provided by the computer software and the iterations it led to, ending with the results and discussion.

To analyse the structural behaviour of the design, the structure was modelled in SAP2000 (*CSI Portugal | SAP2000*, n.d.), a finite element program that allows the user to evaluate the stresses that result from a variety of load types. This program was chosen due to its selection by several engineering and academic organizations. The intention is to convert the properties of the elements and the structure to the mathematical model, and then use the results to verify safety. The verification was done according to the recommendations of the structural design standard ISO 22156:2021 (*ISO*, 2021) , as it was the only international standard for bamboo and showed to be the most recent option (published 03/06/2021).

The model developed holds the following assumptions, amongst others referenced in the IS (International Standard):

- Bamboo is modelled as a linear elastic material through the allowable stress;
- Bamboo culms are conservatively modelled as hollow tubes having cross section dimensions equal to the smallest dimension of the culm;
- Second order effects resulting from imperfect members are considered;
- All joints are assumed to be pinned (hinged);

This chapter also demonstrates all the value suppositions and simplifications taken and used in the model. Furthermore, in ‘Results and Discussion’, the different stresses obtained at the most critical locations, that resulted from the application of the load combinations required by the national building codes.

5.1. International Standards

Conventional construction materials such as concrete and steel were once unconventional and questionable. The approval of these materials was only accomplished by years of experimenting and the accumulation of data through standardized work. The increase of control results in the decrease of variability. For an emerging anisotropic material as bamboo, the standards are largely responsible for enabling the confidence in using it as a reliable alternative, and a variety of thorough international standards are now available.

5.1.1. Test Methods

In 2004, the first bamboo international standard was released by the International Organization for Standardisation (ISO) in cooperation with the International Network for Bamboo and Rattan (INBAR). The effort resulted in the ISO 22157:2004 *Bamboo – Determination of physical and Mechanical Properties* (ISO, 2004c), as well as a *Laboratory Manual* (ISO, 2004a), working as a guide to perform the laboratory tests in ISO 22157. With the intent of taking a step towards making bamboo an "internationally recognised and accepted building and engineering material", this standard became adopted formally by at least eight countries and is known to be used more broadly (D. J. Trujillo & López, 2019; Gauss et al., 2019).

A strongly revised testing standard was further published in 2019 (ISO 22157:2019- Bamboo structures - Determination of physical and mechanical properties of bamboo culms - Test methods (ISO, 2019)). This latest incorporates the following tests: moisture content; density; mass per unit length; compression parallel to fibers; bending, shear and tension both parallel and perpendicular to fibers. Authors argue that other tests are likely to appear in future revisions. Harries et al. (2012) provides a summary of material properties tests available for bamboo.

5.1.2. Grading

Strength grading can be divided into visual and machine grading. The first observes and measures the physical characteristics. Extremely relevant, for example, in measuring the outer diameter and wall thickness of the culms. D. Trujillo & Jangra (2016) state that an increase of 10% in the outer diameter will result in a 24% decrease in bending capacity. Likewise, the wall thickness is highly related to shear and tension resistance perpendicular to the fibers. Machine grading is essential to determine the flexural stiffness, linear mass and external diameter, which can be measured in a simple and economical manner (D. Trujillo & Jangra, 2016). The process of testing, together with grading the culms to use in construction will greatly minimize the risk of building with bamboo. Grading can be done in compliance with ISO 19624:2018- Bamboo structures- Grading of bamboo culms- Basic principles and procedures (ISO, 2018).

5.1.3. Structural design

Also in 2004, ISO 22156:2004 (*Bamboo - Structural Design* (ISO, 2004b)*)* was published. This document can be viewed as a version zero of a structural design approach, given its lack of practical guidance. This standard is very general and is considered to be inconsistent with existing National Standards, although having similar objectives. In 2021, it was published a strongly revised and more detailed structural design document (ISO 22156:2021). It contains complete design equations and is up to date with the new revisions of normative references (ISO 22157:2019 and ISO 19624:2018) (Kaminski et al., 2020). As mentioned, the ISO 22156:2021 was the guiding standard for the design and structural analysis in this document.

5.2. Moso Bamboo

From the vast number of existent bamboo species, few are considered appropriate to use as a structural element. The most frequently used according to the international standard are the following:

- *genus Guadua: G. Angustofolia Kunth, G. Aculeata*
- *genus Phyllostachys: P. edulis (Moso Bamboo), P. meyeri, P. nigra, P. bambusoides*
- *genus Dendrocalamus: D. giganteus, D.asper, D. strictus, D. barbatus G. apus*
- *genus Gigantochloa: G. atter, G. atroviolacea*
- *genus Bambusa: B. blumeana, B. stenostachya, B. oldhami*

These are also the species that have been studied more thoroughly and therefore have the most reliable data.

In the process of choosing a species for this case study, research was made on which could grow in Portugal, considered a mild subtropical country. For this matter, a bamboo nursery based in Alentejo, Portugal was contacted to find if the species known to be fit for structural use existed. Out of the referenced above, Phyllostachys Edulis (Moso) was guaranteed to grow in the nursery.

As mentioned, the material properties of bamboo will vary depending on the place and soil in which it grows. Thus, cautioned measures had to be considered, since no literature on material properties of bamboo growing in Portugal was found. The steps missing to find a reliable producer of structural bamboo in Portugal are harvesting, treating, grading, and testing bamboo, all according to the most recent standards.

The dimensional properties considered in the present work were based on the existing literature of the species Moso, and the mechanical properties mostly on values for the same species determined as required by the standards.

Retaining such variable values can lead to inaccurate design assumptions, reason for which it is of utmost importance to ensure proper grading of the used culms *in situ*. Combining this with mindful design is just as indispensable.

5.3. The Structure

The design of the structure was mostly conditioned by the nature of the material. Not only in terms of the properties of bamboo as a structural element, but also due to the implications of the causes of decay of this organic material. Moreover, the fact that there would be no bending moment transferred between horizontal and vertical elements resulted in a clear necessity of a strong bracing system.

The core idea was to design a residential structure and test its safety according to the recommendations of the new version of the ISO22156, while implementing all of the good practices found in the literature review. The concept did not primarily concern architectural matters as lighting, the distribution of the spaces, nor the highest level of innovation. Although there are infinite possibilities to explore in this realm, for this analysis just the purpose of each space and area was considered.

In the research for similar structures and studies, a project in Lombok, Indonesia to build humanitarian housing after the damage originated from the earthquakes in 2018 was found (*Lombok Bamboo Housing | Ramboll | Archello*; International Bamboo and Rattan Organisation, 2021). This study helped as

inspiration for the design of the structure, although no information about the structural analysis or assumptions for resistance were found.

Figure 23- Lombok humanitarian housing by engineering and design consultancy Rambol, University College London (UCL), and a local NGO (*Lombok Bamboo Housing | Ramboll | Archello*, n.d.).

The decision of including a mezzanine in the structure would make it possible to evaluate the behaviour of bamboo as a structural element for the floor, as well as give a more interesting environment for those using the space.

One of the measures in the section 'Durability by Design' was to extend the roof overhang up to 45º from the bottom of the columns to the edge of the roof, protecting the exposed culms from driving rain. This is not demanded or necessarily advised if the structure is protected with impermeable walls, but for this analysis, the 45º angle was considered. Consequently, a higher structure means not only stronger wind loads but also a longer roof overhang.

The design process began by discussing the geometry of the base of the structure. Since the residence would have two levels, it made sense that the height of the vertical elements would be 2,5m high. This way, the ground level would have a decent ceiling height, keeping in mind that the structural frame would be elevated from the ground around 30cm, as durability measures suggest. A spacing of 2m between columns seemed valid as well.

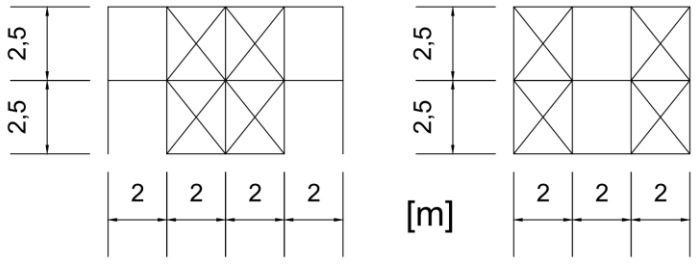

Figure 24- Front views of the sides of the base structure.

These considerations resulted in an area of 48m^2 in the bottom floor and another 24m^2 in the mezzanine. As for the pitch angle of the roof, a value that led to round values in the plan view of the roof was desired,

not over compromising the lighting and also not extending the roof too far away from the structure, which resulted in an angle of 18º.

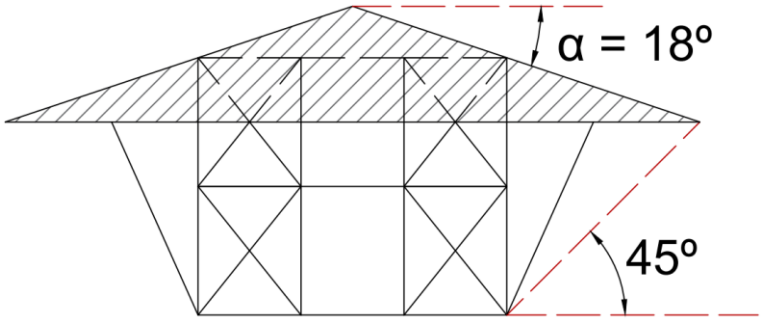

Figure 25- Pitch angle of the roof.

For the roof elements, the plan started as in the figure below, although some minor alterations were done in the analysis of the stresses, described further.

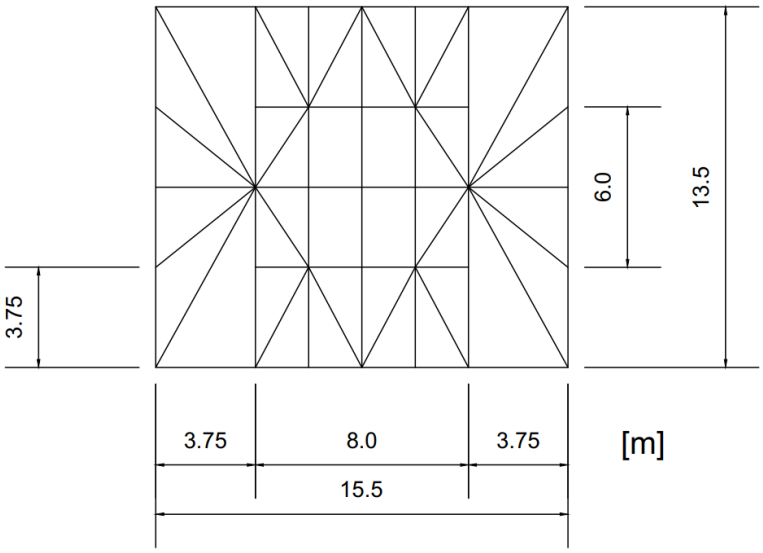

Figure 26- Plan of the roof structure.

Looking at the 3,75 m extensions of the roof in the plan above, it was easy to foresee that some support could be necessary in that area. Diagonals connecting the foundations to the roof were added later on, in the nodes of the roof that responded best to the stresses shown in the program.

5.4. Loads

5.4.1. Dead Loads and Live Loads

The identification of the actions was made using Eurocode 1 (Portuguese Norm NP EN 1991-1-1, 2009). The roof was taken as of category 'H', which is defined as not accessible, except for maintenance and repair operations. This leads to a recommendation of a live load of 0,4 kN/m^2, distributed by all of the roofing area, or a punctual load of 1 kN applied in the least favourable point, applied separately.
The self weight of the bamboo is automatically considered in the computer program.
Given the mentioned necessity to keep bamboo dry, a profiled steel plate on top of the roof was also considered in the analysis. This plate will transmit its own weight, the live loads and the external forces to the top roofing elements.
The profiled steel plate was chosen from the catalogue of a Portuguese company by the name of 'O Feliz' (*O FELIZ*, n.d.), since it presented tables to assist the choice of the plate according to the upwards and downwards wind design loads, considering the Eurocode standards. After analysing these loads and considering a simply supported plate, the plate selected presented a 0,5 mm thickness and a weight of 4,51 kg/m^2, equivalent to 0,044 kN/m^2.
In short, the structure is subjected to the following dead and live loads:

- Self weight of the bamboo poles – automatically considered in the program;
- Steel plate self weight – approximately 0,05 kN/m^2;
- Roof live load, q_k – 0,4 kN/m^2 distributed by all the roof;
- Roof live load, Q_k– 1 kN/m^2 in the least favourable point;

The roof loads were introduced in the program as punctual loads at the end nodes of the bamboo elements, using the same method as for the wind action presented in the following chapter. The full extent of the calculations can be found in the annex.

5.4.2. Wind Action

To consider wind action, the European codes were used to find the corresponding loads and combinations to apply. Since the roof area was designed considerably large when compared to the base of the structure, the wind effect is extremely important to consider. For this reason, in the present chapter the sequence of equations used to determine the loads and the simplifications taken are described in a more detailed way. All the following expressions were found in the work of Mendes & Oliveira Pedro, 2020 or directly from the Eurocode (*Eurocode 1: Wind Actions*, 2005).

5.4.2.1. Determination of the Peak Velocity Pressure

To begin, the basic wind velocity, which is associated with an annual probability of being exceeded equal to 0,02 (return period of 50 years), was determined with the following formula:

$$v_{\mathrm{b}} = c_{\mathrm{dir}} \cdot c_{\mathrm{season}} \cdot v_{\mathrm{b},0} \tag{1}$$

v_{b} is the basic wind velocity, defined as a function of wind direction and time of year at 10 m above ground of terrain category II, which is described further.

c_{dir} is the directional factor. The recommended value is 1,0.

c_{season} is the season factor. The recommended value is also 1,0.

$v_{\mathrm{b},0}$ is the fundamental value of the basic wind velocity. The characteristic 10 minutes mean wind velocity, irrespective of wind direction and time of year, at 10 m above ground level in terrain of category II.

In order to quantify $v_{\mathrm{b},0}$ in Portugal, the country is divided in two zones. The considered piece of land for the construction of the bamboo structure is not in the coast of the country, and is therefore in zone A, which is associated with a $v_{\mathrm{b},0} = 27\mathrm{m}/s$ (return period of 50 years).

The medium velocity of the wind depends not only on the height above ground in a specific location, but also on terrain conditions. To take it into account, the locations are sorted into different categories. The category II is described as an area with low vegetation such as grass and isolated obstacles (trees, buildings) with separations of at least 20 obstacle heights. This was the type of area considered to build the structure. This will be relevant in determining the roughness factor, $c_r(z)$, calculated using:

$$c_r(z) = 0{,}19 \cdot \left(\frac{z_0}{z_{0,II}}\right)^{0{,}07} \cdot \ln\left(\frac{z}{z_0}\right) \quad \text{for} \quad z_{\min} \leq z \leq z_{max} \tag{2}$$

where:

z_0 is the roughness length

$z_{0,II}$ is the roughness length in terrain category II (0.05).

As category II leads to values of $z_0 = 0.05\ m$ and $z_{min} = 3\ m$, the roughness factor result is the following:

$$c_r(z) = 0{,}19 \cdot \left(\frac{z_0}{z_{0,II}}\right)^{0{,}07} \cdot \ln\left(\frac{z}{z_0}\right) = 0{,}19 \cdot \ln\left(\frac{6}{0.05}\right) = 0{,}91 \tag{3}$$

The mean wind velocity at a height z ($v_{\mathrm{m}}(z)$) above the terrain depends on the terrain roughness, orography and also on the basic wind velocity, v_b, calculated above, and was estimated using the formula:

$$v_{\mathrm{m}}(z) = c_{\mathrm{r}}(z) \cdot c_{\mathrm{o}}(z) \cdot v_b = 0.91 \cdot 27 = 24{,}6\frac{m}{s} \tag{4}$$

where:

$c_{\mathrm{r}}(z)$ is the roughness factor. Accounts for the variability of the mean wind velocity at the site of the structure.

$c_{\mathrm{o}}(z)$ is the orography factor, taken as 1,0.

Regarding the turbulence intensity at height z ($I_v(z)$), which is defined as the standard deviation of the turbulence divided by the mean wind velocity, the calculation was the following:

$$I_v(z) = \frac{1}{c_o(z) \cdot \ln\left(\frac{z}{z_0}\right)} = 0{,}21 \quad (5)$$

The peak velocity pressure at height z ($q_p(z)$), which includes mean and short-term velocity fluctuations, was determined according to the formula:

$$q_p(z) = c_e(z) \cdot q_b = 771{,}6\ \mathrm{N}/m^2 \quad (6)$$

where:

$c_e(z)$ is the exposure factor, calculated in Equation (7) presented below.

q_b is the basic velocity pressure, calculated in Equation (8) written below.

$$c_e(z) = [1 + 7 \cdot I_v(z)] \cdot c_r^2(z) \cdot c_0^2(z) = 2{,}04 \quad (7)$$

$$q_b = \frac{1}{2} \cdot \rho \cdot V_m^2(z) = 378.2\ \mathrm{N}/m^2 \quad (8)$$

where:

ρ is the air density, which depends on the altitude, temperature, and barometric pressure to be expected in the region during wind storms. The recommended value is 1,25 kg/m^3.

After knowing the peak velocity pressure, only the pressure coefficients for the external and internal pressure (c_{pe} and c_{pi}, respectively) are lacking to be able to determine the wind pressure acting on the external and internal surfaces of the structure (w_e and w_i, respectively), as they are determined by:

$$w_e = q_p(z_e) \cdot c_{pe} \quad ; \quad w_i = q_p(z_i) \cdot c_{pi} \quad (9)$$

5.4.2.2. Wall Pressures

The pressure coefficients are different for the walls and for the roof. For the walls, recommended values will depend on the geometry of the building. For the height/width ratio of the structure under analysis, the recommended values interpolated from Eurocode (*EC 1: Wind Actions*, 2005) can be found below. Note that the values correspond to $c_{pe,10}$ (used for the design of the overall load bearing structure of buildings).

Table 1- Design pressure values for the walls.

h/d	$C_{pe,10}$ - Windward	$C_{pe,10}$ - Leeward
2	0,8	-0,55

These area loads caused by the wind were attributed in the program by isolated forces, as Figure 27b) suggests. The forces distributed in the wall areas were multiplied by a value corresponding to the influence area.

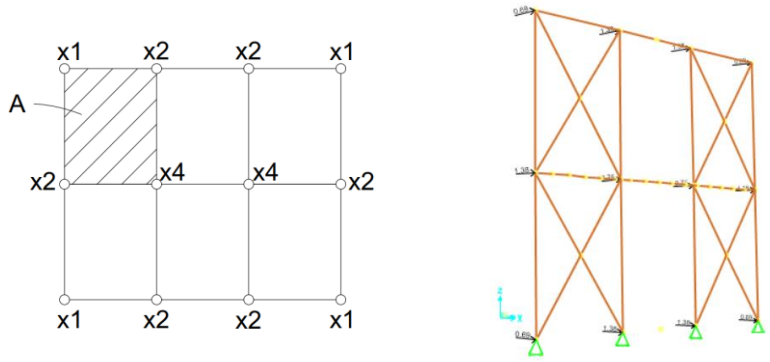

(a) (b)

Figure 27- Wind forces applied to walls.

5.4.2.3. External Pressure

Regarding the roof, the Eurocode advises a specific distribution of pressures for each type of shape. Since the roof design is hipped, the load distribution is sorted in the separated areas in Figure 28a). As a simplification, these areas were adjusted to the roofing elements Figure 28b) to facilitate the introduction of the loads in the computer program. These small geometric adjustments were done taking into consideration the pressure values of each specified letter area. As a result, a conservative approach was guaranteed.

The pressures are also sorted according to the wind direction. When the wind in facing one of the longer sides of the building it is described as $\theta=0^{o}$, and for the perpendicular direction as $\theta=90^{o}$, as they represent the most onerous directions for a structure (Figure 28).

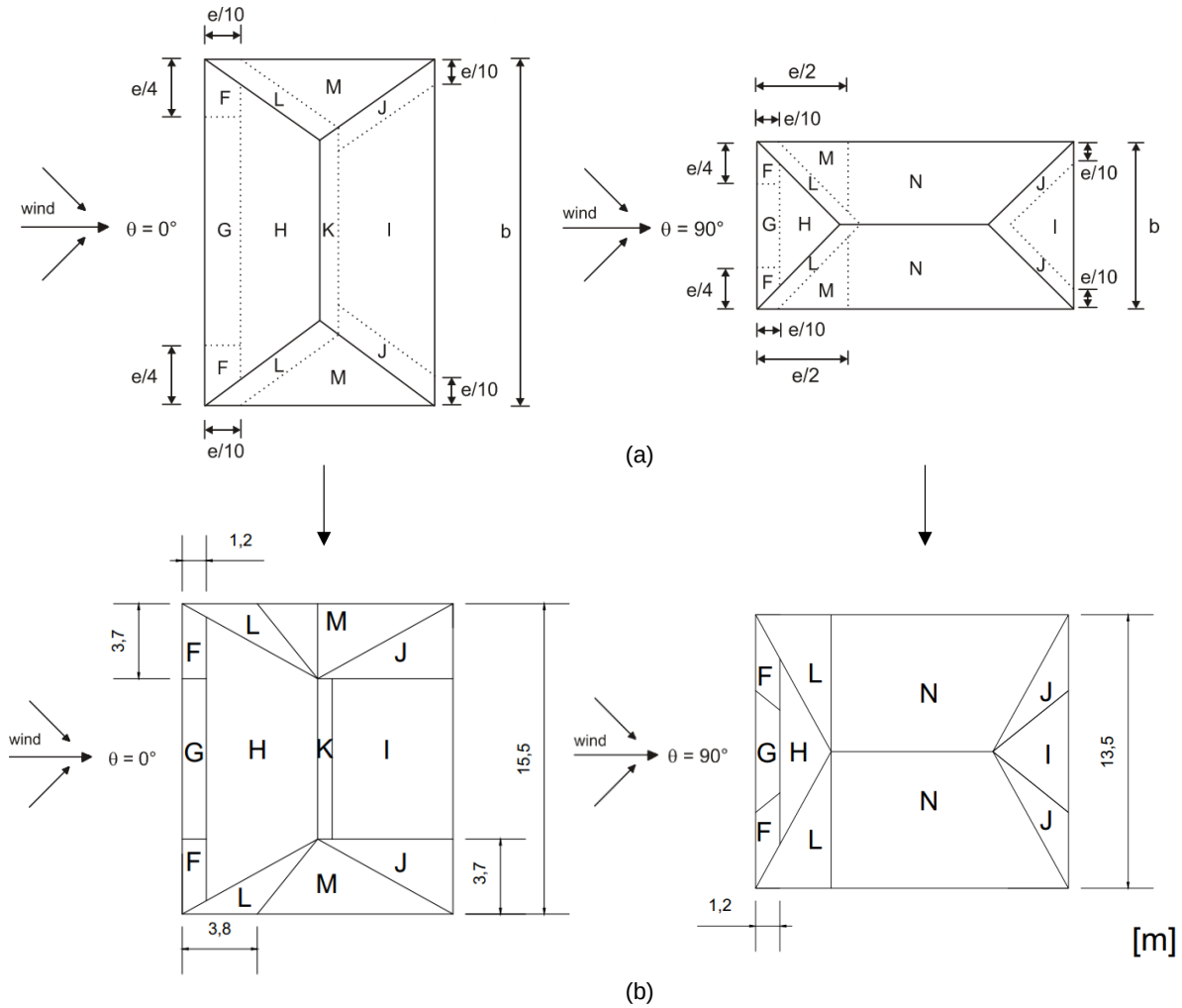

Figure 28- a) Zone distribution for hipped roofs to account wind action (*Eurocode 1: Wind Actions*, 2005); b) simplified distribution adopted in the present analysis.

The external pressure coefficients present in each area depend on the pitch angle of the roof. As illustrated in Figure 25, the angle is equal to 18º. The values in Table 2 were interpolated from the table provided in the Eurocode (*Eurocode 1: Wind Actions*, 2005) for the specific angle.

Table 2- External pressure coefficients for hipped roofs with α=18º.

External Pressure Coeficients for Hipped Roofs (Cpe)									
	F	G	H	I	J	K	L	M	N
18º	-0.82	-0.74	-0.28	-0.48	-0.94	-1.06	-1.4	-0.64	-0.28
	0.26	0.3	0.24	-	-	-	-	-	-

These pressures multiplied by the peak velocity pressure at height z as in Equation (9, we obtain the following load values in kN/m^2:

Table 3- External loads for α=18º.

External Loads (KN/m^2)									
	F	G	H	I	J	K	L	M	N
18º	-0.63	-0.57	-0.22	-0.37	-0.73	-0.82	-1.08	-0.49	-0.22
	0.20	0.23	0.19	-	-	-	-	-	-

The positive values of the external forces were not considered, as they represent a less critical approach.

Knowing the loads and their distribution by the zones illustrated in Figure 28b), it is important to consider the load path through the elements of the structure. In Figure 29, the black lines correspond to the elements in the bottom face of the roof, holding the red elements that are on top of the roof, in contact with the profiled steel plate. The green diagonal elements are also in the bottom, yet they were considered only to account for the bracing of the roof and did not have an impact on the resistance to wind action in this calculation.

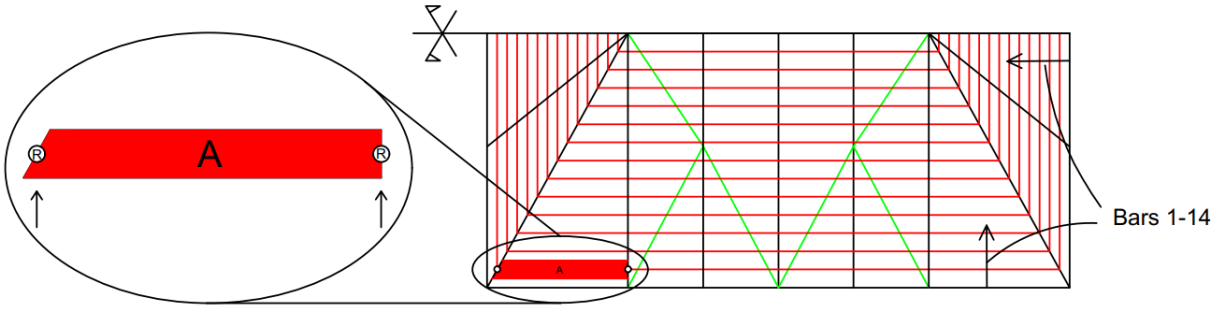

Figure 29- Roof elements and load reactions scheme.

So, taking the load distribution considered, it was decided to firstly determine the influence area for each element. Each of these areas multiplied by the correspondent load distributions described in Table 3 and divided by two, give us the reactions in both of the supports (the bottom elements), as in the left side of Figure 29.

$$R_{e,i} = \frac{A_i \times c_{\mathrm{pe,i}}}{2} \; and \; R_{i,i} = \frac{A_i \times c_{\mathrm{pi,i}}}{2} \; (KN) \qquad (10)$$

where:

A_i Influence area correspondent to element *i.*

$c_{\mathrm{pe,i}}$ Downward load cpe (kN/m²) in element *i* (Table 3).

$c_{\mathrm{pi,i}}$ Upward load cpi (kN/m²) in element *i* (Table 3).

$R_{e,i}$ Reaction in the supports of element *i* under external loads.

$R_{i,i}$ Reaction in the supports of element *i* under internal loads.

Since the wind loads act perpendicularly to the roof, the area elements considered were obtained from the 3D model and not from the plan of the roof.

The two reactions R present in each connection were added together. For this purpose, the primary elements and areas were divided as in Figure 30. These bottom roofing elements were numbered, and the areas between these elements were named depending on their position in the roof ("C"=centre, "D"= diagonal) and according to the wind direction ("W"=windward, "L"=Leeward). Using this nomenclature, the sums were made and the final reactions along each numbered element were calculated.

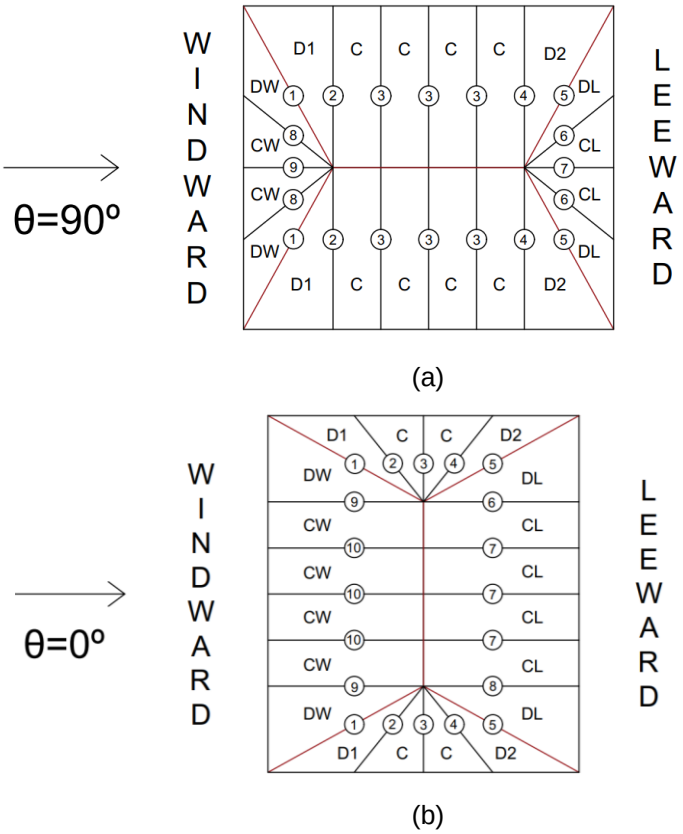

Figure 30- Designation of elements and zones for a) θ=0º and b) θ=90º.

In the annex are the tables of the results and calculation process using Excel, showing firstly the determination of the reactions for each individual element, and then the sum of the two reactions in each connection, resulting in the loads transferred to the bottom elements. These last values are the loads introduced in the computer software.

To authenticate the calculations, the summation of the totality of wind loads was verified. Meaning, the values of the loads in Table 3 times the areas in Figure 28b) (i) were compared to the sum of the isolated loads in Table 4 (ii). The results are summarised in the table below. The complete calculation can be found in the annex.

Table 4- Load comparison from different calculation methods.

	For θ=0º	For θ=90º
(i) Sum of FxA (kN)	-111.31	-86.71
(ii) Sum of Isolated Loads (kN)	-111.30	-86.62
i/ii	1.00	1.00

As the results demonstrated to be of the same magnitude within the conservative approach, the loads were considered valid to proceed with the analysis.

5.4.2.4. Protruding Roof Corners

The Eurocode states that for protruding roof corners, the pressure to consider on the underside of the roof overhang is equal to the pressure for the zone of the vertical wall that is directly connected to the protruding roof (*Eurocode 1: Wind Actions*, 2005). On the top side the pressures are defined as previously.

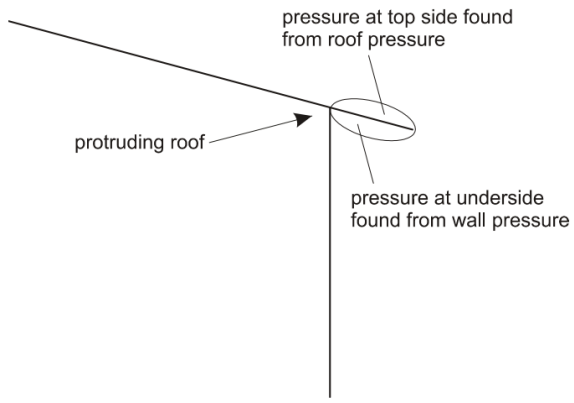

Figure 31- Illustration of pressures for protruding roofs according to the Eurocode.

Since the wall pressures (defined in Table 1) resulted in an upward force exclusively on the overhang roof in the leeward wall, it was decided to add only the forces from this side, conservatively. The calculation of the overhang forces was done in the same system, using isolated loads that could be posteriorly added to the original wind loads. Calculation of the forces in the annex.

Given the extension of the roof overhang, it was expected that these loads would represent a significant difference. This proved to be true, as the sum of the isolated loads in the roof due to the protruding roof corners resulted in upward loads of 91,9 kN for θ=0º and 32.4 kN for θ=90º.

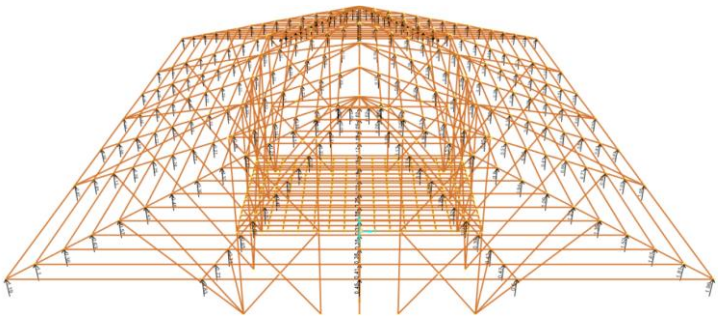

Figure 32- Representation of the joint loads of the wind action inserted in the computer program.

The final wind loads assigned to the load patterns defined as “Wind-Roof θ=0º” and “Wind-Roof θ=90º” in the software SAP2000 now also contemplated the overhang roof loads.

5.4.2.5. Internal Pressure

As for the internal pressures, the Eurocode (*Eurocode 1: Wind Actions*, 2005) provides a number of different rules depending on the area and disposition of the openings and leakages (windows, ventilators, etc.) on the faces of the building considered. For the cases where it is not possible or justified to go into detail, the code states “c_{pi} should be taken as the more onerous of +0,2 and -0,3”. Since those details of openings were not yet considered, the values just mentioned were taken. Once again, only the upward load represents a relevant and critical addition. The Eurocode assigns the direction of the pressure in the following way:

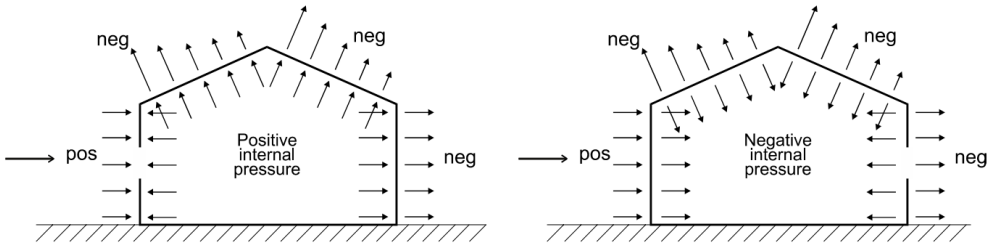

Figure 33- Description of the direction of negative and positive pressures.

The upward load of 0,2 kN/m was multiplied by the peak velocity pressure (Equation (9) and then by the influence area around each node. Due to the motive of the internal pressures, the loads were applied exclusively in the area above the structure, as Figure 34 suggests.

Table 5- Calculation of the internal loads introduced in the software for the roof.

Cpi	Wi (KN/m^2)	A (m^2)	R (KN)
0.2	0.154	1.016	0.157

The loads of the internal pressures in the walls of the structure were introduced in the same format as the wind loads. The internal pressures for θ=0º are illustrated below.

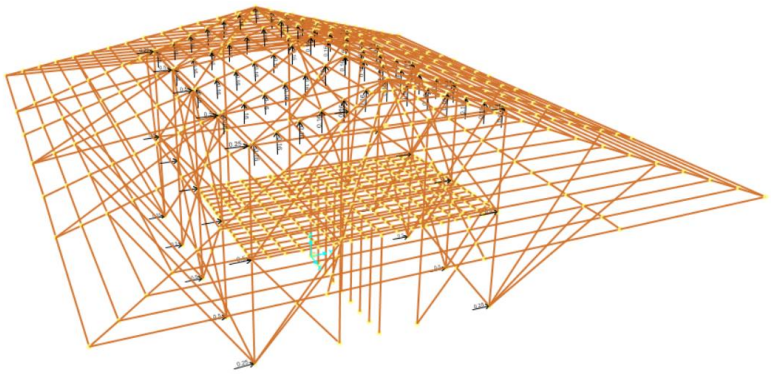

Figure 34- Illustration of the assignment of internal loads in SAP2000.

The internal and external pressures shall be considered simultaneously. Therefore, the internal loads (load case named “Cpi”) were added to all the combinations that include the remaining wind loads, as demonstrated below.

5.4.3. Load Combinations

The load combinations were defined with the intention of maximizing either the upward loads or the downward loads. Permanent loads in the absence of wind action were also considered. The table below details loads and coefficients for each combination.

Table 6- Load combinations and load case scale factors.

COMB_0_1.5	Scale Factor
Wind-Wall θ=0º	1.5
Wind-Roof θ=0º	1.5
Cpi	1.5
Dead	1
Steel Plate	1

COMB_0_1	Scale Factor
Wind-Wall θ=0º	1
Wind-Roof θ=0º	1
Cpi	1
Dead	1.35
Steel Plate	1.5
Live	1.5

COMB_90_1.5	Scale Factor
Wind-Wall θ=90º	1.5
Wind-Roof θ=90º	1.5
Cpi	1.5
Dead	1
Steel Plate	1

COMB_90_1	Scale Factor
Wind-Wall θ=90º	1
Wind-Roof θ=90º	1
Cpi	1
Dead	1.35
Steel Plate	1.5
Live	1.5

Dead+Live	Scale Factor
Dead	1.35
Live	1.5
Steel Plate	1.5

Given the strength of the upward loads, the combinations “COMB_0_1” and “COMB_90_1” did not lead to any maximum stress in the analysis. The combinations used for the dynamic analysis can be found in the correspondent chapter.

5.5. Design Values

The design values in the present text were all determined according to the structural design standard ISO 22156:2021, using characteristic values that correspond to the specific requirements. The values used were confirmed to be of the same magnitude as others from similar studies.

Given the conditions where the structure would be found, this study considers a service class 2 for the design, characterised by an equilibrium moisture content in the bamboo not exceeding 20%. Note this is “representative of indoor unheated or uncooled environments in most locations, except those with relative humidity regularly or for prolonged periods exceeding 85%”.

5.5.1. Diameter and Wall Thickness of the Culms

Previous research shows that a diameter of 100 mm with a wall thickness of 10 mm is reasonable to consider, therefore, those were the values chosen for the analysis. As bamboo does not have a continuous section, the grading of the culms used *in situ* is essential, where relevant aspects like the tapering of the culms and wall thickness variation with height are considered. The following table shows some typical values for the outer diameter and wall thickness:

Table 7 - Diameters and wall thickness values of mature Moso bamboo.

Authors	Outer Diameter (mm)	Wall Thickness (mm)	Location
(Kaminski, Laurence, et al., 2016)	120 - 180	-	-
(Harries et al., 2017)	60 - 120	6 - 17	-
(Wang et al., 2019)	120	11	Zhejiang, China
(Wang et al., 2020)	115	11	Zhejiang, China
(Gauss et al., 2019)	80 - 100	6 - 9	São Paulo, Brazil
(Gauss et al., 2020)	70 - 90	6.5 - 10	São Paulo, Brazil
(Deng et al., 2016)	>100	-	Jiangxi, China

The area of the cross section, which is a function of the outside diameter and wall thickness, will have a very influential effect in the strength domain.

To determine the section area, the ISO 22156:2021 states both the culm diameter D and nominal culm wall thickness δ have the same approach to account variability: if the difference between ends is fewer than 10%, the average value shall be used. Otherwise, the smallest value of the two must be assumed.

This, if the culms have not been graded previously in agreement with ISO 19624. The formula to determine the cross sectional area is:

$$A = \left(\frac{\pi}{4}\right) \times [D^2 - (D - 2\delta)^2] \quad (11)$$

The option of an outside diameter of 0,1m and a wall thickness of 0.01m results in a cross section area of 2,827×10^{-3} m^2. Moreover, the moment of inertia of a single culm in line with the international standard shall be calculated using:

$$I = \left(\frac{\pi}{64}\right) \times [D^4 - (D - 2\delta)^4] \quad (12)$$

The result of the inertia for these geometric properties is 2.898^{-6} m^4.

5.5.2. Modulus of Elasticity

The Modulus of Elasticity (MOE) is crucial to correctly evaluate the deformations in service conditions. D. J. Trujillo & López (2019) indicate that in the Colombian Standard NSR10 (AIS, 2010), MOE values are surprisingly low, justifying these 'apparent' values as a concern that the state of the art in connection design did not allow for reliable predictions of slippage. The ISO:22156:2021 likewise strongly reduces the mean value of MOE as presented in Equation (13, having different reductions depending on service classes and temperatures.

To have an idea of the typical mean values of MOE for this species, some results of available literature were considered: Gauss et al. (2020) and Gauss et al. (2019) MOE characteristic values range between 15.19 GPa and 18.04 GPa. These results were deducted from the mean values according to the standard deviation, which was relatively low. Both studies quoted Dixon et al., (2015) results of MOE values in bending of 16.680 GPa with samples of similar density. Correal D. & Arbeláez C. (2010) find average results for axial modulus of elasticity in compression and bending tests (ISO 22157) around 17GPa. Habibi et al., (2015) and Godina & Lorenzo (2015) found lower values, yet never below 11 GPa. (Lorenzo et al., 2020) conducted tests adopting Chinese industry standard JG/T 199-2007 which led to a value of 11.93 GPa. Strain values in the references above were determined mostly from Digital Image Correlation (DIC) analysis.

Note that the ISO 22157:2019 does not include a small coupon bending test. D. Trujillo et al. (2017) considers the full culm bending test present in the standard is appropriate for grading based on member flexural capacity of the tested culm. However, it is not a materials evaluation test, and should not be used in a stress-based design as it does not provide a meaningful stress (Gauss et al., 2020, Gauss et al., 2019). Therefore, the bending modulus of elasticity and bending capacity results are often determined by the small coupon bending test (commonly performed according to the standard ASTM D7264). However, this will not interfere with the formula provided by ISO22156:2021 to determine the design value of MOE, because it is based on the mean characteristic compressive modulus of elasticity:

$$E_{\mathrm{d}} = E_k \times C_{DE} \times C_T \quad (13)$$

Where:

E_k is the mean characteristic compressive modulus of elasticity with 75 % confidence determined from ISO 22157. In ISO 12122-1, the value is denoted $E_{\mathrm{mean},0,75}$.

C_{DE} is the modification factor for service class and load duration given in Table 8.

C_T is the modification factor for service temperature. Assuming the temperature values will not pass 38º, the recommended value is 1,0.

This study uses characteristic values of MOE from the work of Gauss et al. (2020), similarly to the characteristic values of the strengths regarded further. This, because the result of the mean characteristic compressive MOE in this study (Ec = 18,040 MPa) was established with 75% confidence and the compression test according to the ISO 22157, as it is required by the standard.

The load duration factor for modulus, C_{DE} for Class 2 is given by:

Table 8- Load duration factor for modulus.

Load Duration	Service Class 2
permanent and long term applied load	0,45
transient loads	0,95
instantaneous loads (wind and seismic)	1,00

This means that for permanent loads, the MOE value taken in this study was 8.118 MPa. Conservatively, this was the value used in all of the calculations since the characteristic value (Ec = 18,040 MPa) was higher than average of the values in the literature review.

5.5.3. Weight per Unit Value

To select a density value to introduce in the software, studies on bamboo density were evaluated to find a reasonable consideration. Some values can be found in Table 9, which led to an average value close to 700 kg/m^3. The value considered was 8 kN/m^3, which is equivalent to 815,77 kg/ m^3.

Table 9 - Density values of mature Moso bamboo studied by respective authors.

Authors	Density (kg/m^3)
(Dixon et al., 2015)	400 - 850
(Deng et al., 2016)	655 - 799
(Lorenzo et al., 2020)	684
(Dixon & Gibson, 2014)	630
(Zhuo Ping Shao et al., 2010)	710
(Gauss et al., 2019)	810

5.6. Allowable Strengths

This chapter focuses on identifying the design strengths and properties necessary to implement the verifications required in the standard.

The design methodology approached by the ISO 22156:2021 to ensure the safety and performance of a structure is based on allowable stress design (ASD). Amongst several relevant recommendations, the standard sees the allowable design strength should be taken as:

$$f_i = f_{ik} \times C_R \times C_{DF} \times C_T \left(\frac{1}{FS_{\mathrm{m}}}\right) \quad (14)$$

f_i is the allowable design strength.

f_{ik} is the 5th percentile characteristic strength with 75% confidence. In ISO 12122-1, the value is denoted fi,0,05,0,75.

C_R is the member redundancy factor. For load-bearing members $C_R = 0.90$. This was the value considered for all of the elements in the structure.

C_{DF} is the modification factor for service class and load duration. For service class 2, the values are shown in Table 10.

FS_{m} is the material factor of safety given in Table 11.

Table 10- Load duration modification factor for service class 2 according to ISO 22156:2021.

Load Duration	Service Class 2
permanent and long term applied load	0,55
transient loads	0,65
instantaneous loads (wind and seismic)	0,85

Table 11- Material factor of safety values (FS_{m}) according to ISO 22156:2021.

Nc (Compression)	Nt (Tension)	M (Bending)	V (Shear)
2,0	2,0	2,0	4,0

The previous adjustment factors all act upon the characteristic material strength. Therefore, this is the most relevant step to determine the allowable strength of an element. The standard shows that it is possible to infer the characteristic value by grade using specific guidance from ISO 19624 or determined from the testing standard ISO 22157.

For this analysis, the values used for the characteristic strength were taken from a study that tested 140 Moso bamboo culms from a supplier near São Paulo, Brazil (Gauss et al., 2020). The culms tested were aged between 3 and 5 years old, the diameters ranged between 70 and 90 mm, and the oven dry density prior to treatment was 760 kg/m^3. The values from this study were preferred to others as a result of the characteristic values of compression, tension, shear, and bending having been calculated according to ISO 22157-19. Moreover, the values (shown below) are defined as the 5th percentile value determined with 75% confidence, as required.

- f_{ck} = 49,5 MPa, f_c being the compression strength parallel to fibres.
- f_{vk} = 15,4 MPa, f_v being the shear strength.
- f_{tk} = 220 MPa, f_t being the tension strength parallel to fibres.
- f_{bk}= 183 MPa, f_b being the bending strength parallel to fibres, although in ISO 22156 it is referred as f_{mk}.

Ideally, there will be a solid connection between the standards of testing, grading, and structural design for the bamboo used in construction. As it has been discussed, the characteristic values may vary with a variety of circumstances, so the level of confidence building with bamboo will mostly improve with this type of literature and development. Recognizing this, the following calculations result in the final strength values to be evaluated aside the stresses.

For permanent loads:

$$f_c = f_{ck} \times C_R \times C_{DF} \times C_T \left(\frac{1}{FS_{\mathrm{m}}}\right) = 49.5 \times 0.9 \times 0.55 \times 1 \times \frac{1}{2} = 12.25\ MPa \qquad (15)$$

And for instantaneous loads:

$$f_c = f_{ck} \times C_R \times C_{DF} \times C_T \left(\frac{1}{FS_{\mathrm{m}}}\right) = 49.5 \times 0.9 \times 0.85 \times 1 \times \frac{1}{2} = 18.93\ MPa \qquad (16)$$

The remaining strength values were calculated in a similar manner. To obtain the resistances in kN, the tested values were multiplied by the area of the cross section, obtaining the results present in the table below.

Table 12- Strength values of compression, tension, bending and shear.

fi	fik	Permanent		Instantaneous	
	MPa	MPa	kN	MPa	kN
fc (compression)	49.5	12.25	34.63	18.93	53.53
ft (tension)	220	54.45	153.93	84.15	237.89
fm (bending)	183	45.29	2.63	70.00	4.00
fv (shear)	15.4	1.91	5.39	2.95	8.33
MOE	18,040	8,118	-	18,040	-

Before beginning with the analysis of the stresses for each load combination, it is important to keep in mind particular verifications quoted in the standard.

5.6.1. Compressive Capacity Accounting Buckling Behaviour and Crushing Capacity

The compressive capacity from geometric and material properties is calculated using:

$$N_{\mathrm{cr}} = \frac{P_{\mathrm{c}} + P_{\mathrm{e}}}{2c} - \sqrt{\left(\frac{P_{\mathrm{c}} + P_{\mathrm{e}}}{2c}\right)^2 - \frac{P_{\mathrm{c}} P_{\mathrm{e}}}{c}} \quad , \quad with \quad c = 0{,}80 \tag{17}$$

where

P_{e} is the buckling capacity defined in (19);

P_{c} is the crushing capacity which shall be determined by:

$$P_{\mathrm{c}} = f_{\mathrm{c}} \times \Sigma A \tag{18}$$

where

f_{c} is the allowable compression strength parallel to fibres given in Table 12;

ΣA is the sum of the cross sectional areas of the individual culms comprising the member.

Regarding buckling capacity of a compression member (P_{e}), the ISO 22156:2021 states it shall be calculated by the equation:

$$P_{\mathrm{e}} = \frac{n\pi^2 E_{\mathrm{d}} I_{min} C_{bow}}{(KL)^2} \tag{19}$$

where

n is the number of culms comprising the member;

E_{d} is the design modulus of elasticity given in Equation (13;

I_{min} is the minimum moment of inertia, defined in Equation (12), of the individual culms comprising the member;

KL is the effective compression member length, where L is the length of the element and K is the effective length coefficient. The ISO22156:2021 states that for laterally restrained elements that are pinned in both ends, K should be taken as 1,1;

C_{bow} is a reduction factor to account for an initial bow in the culms comprising the compression member defined in (20.

$$C_{\text{bow}} = 1 - \left(\frac{b_0}{0{,}02}\right) \tag{20}$$

where

b_0 is the maximum bow at mid height of any culm comprising a compression load bearing member C_{bow} given by:

$$b_{\text{o}} = \frac{b_{max}}{L} < 0{,}02 \tag{21}$$

where:

b_{max} is the maximum perpendicular distance from the centre of the culm cross section to the chord drawn from the centres of the ends of the piece of bamboo.

L is the length of the member.

For C_{bow} , the initial idea was to use the maximum allowed value of b_{o}, maximizing C_{bow} and minimizing the value of P_{e} as well as N_{cr}, conservatively. This is not possible since the closer b_{o} is to $0{,}02$, the closer C_{bow} is to zero. This implies that a review on this chapter of the standard may be needed. The solution was found in using $b_{max} = L/250 \Leftrightarrow b_{\text{o}} = 0{,}004 \Leftrightarrow C_{\text{bow}} = 0{,}8$, independently of the value of length of the member.

5.6.2. Lateral Restraint Of Compression Member

Concerning the lateral restraint of a compression member, the standard states that the bracing elements shall be capable of resisting a force F_{resc} oriented perpendicular to the principal axis of the member about which restraint is being calculated. It so happens that the bracing elements present in the structure have not only the purpose of accounting for the buckling of vertical elements but also (and primarily) of resisting wind and earthquake loads. Therefore, the bracing elements are capable of resisting significantly higher loads than F_{resc} .

5.6.3. Combined Axial And Flexural Loads

For combined axial and flexural loads, the standard states that the members shall respect the failure criteria of Equations (22 and (23, for compression and tension respectively.

$$\frac{N_{\text{cd}}}{N_{\text{cr}}} + \frac{BM_{\text{cd}}}{M_{\text{r}}} \leq 1{,}0 \tag{22}$$

$$\frac{N_{\text{td}}}{N_{\text{tr}}} + \frac{M_{\text{cd}}}{M_{\text{r}}} \leq 1{,}0 \tag{23}$$

where

N_{cd} is the design compression force;

M_{cd} is the design bending force;

N_{tr} is the tensile resistance;

N_{cr} is the compression resistance defined in Equation (17;

N_{td} is the design tensile force;

M_{r} is the moment resistance;

B is the moment amplification factor given by Equation (24.

$$B = \left[1 - \frac{N_{\mathrm{cd}}}{P_{\mathrm{e}}}\right]^{-1} \tag{24}$$

5.7. Results and Discussion

Firstly, the design of a bamboo structure and the species selected for the study were addressed. Later, the actions that the structure is submitted to according to national standards and the verifications required from the bamboo structural design international standard were detailed. The stress results obtained from the computer program and the subsequential verifications are discussed in the current section, as well as the iterations implemented.

The stresses derived from each load case were exported to Excel, as well as the results for each combination (previously described in Table 6) to interpret the data. For each stress, the most significant values on the most critical sections are described.

The verifications described in the previous chapter are summarized in the following table:

Table 13- Summary of verifications implemented.

Compression	Shear	Bending
$N_{ed} < N_{\mathrm{cr}} = \frac{P_{\mathrm{c}} + P_{\mathrm{e}}}{2c} - \sqrt{\left(\frac{P_{\mathrm{c}} + P_{\mathrm{e}}}{2c}\right)^2 - \frac{P_{\mathrm{c}} P_{\mathrm{e}}}{c}}$	$V_{ed} < V_{rd} = f_v \times A$	$M_{ed} < M_{rd} = f_m \times W$
Compression + Bending	**Tension**	**Tension + Bending**
$\frac{N_{\mathrm{cd}}}{N_{\mathrm{cr}}} + \frac{B M_{\mathrm{cd}}}{M_{\mathrm{r}}} \leq 1{,}0$	$T_{ed} < T_{rd} = f_t \times A$	$\frac{N_{\mathrm{td}}}{N_{\mathrm{tr}}} + \frac{M_{\mathrm{cd}}}{M_{\mathrm{r}}} \leq 1{,}0$

Analysing frequencies and displacements returned from running the first vibration modes in the program, it became evident that such a prolonged roof needed some stabilizing elements, as suspected. For that reason, some diagonals were added connecting the foundations to the roof. The point in which these

diagonals were connected to the roof was determined to minimize the values of the stresses. At this stage, the stress values in the frames were exported and analysed.

5.7.1. Compression

When designing the diagonal elements, it was predictable that given their length, the compression verification was likely to present issues due to buckling behaviour, which was confirmed to be true. In the image and table below are exposed which diagonals were overstressed, and the comparison of results, respectively.

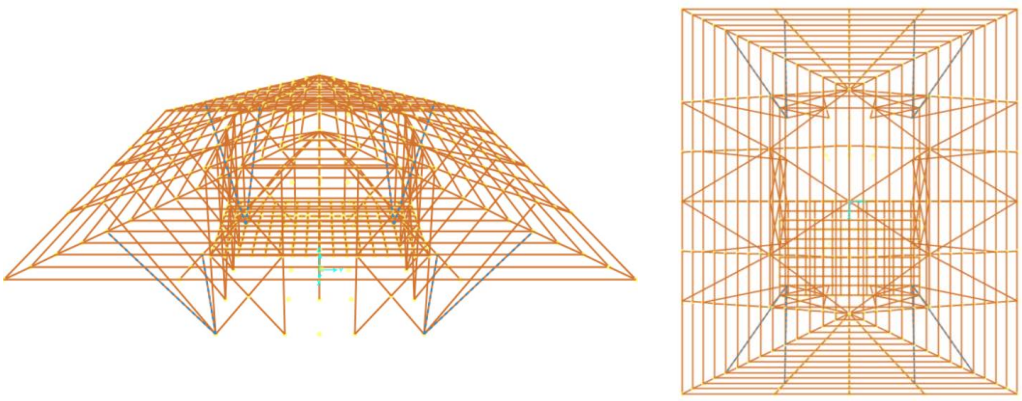

Figure 35- Over-stressed frames.

Table 14- Summary of results of overstressed frames ($N_{\mathrm{cd}} > N_{\mathrm{cr}}$ or $\mathrm{P} > N_{\mathrm{cr}}$).

Frame	Station	OutputCase	P (KN)	L (m)	Cbow	Pe (KN)	Ncr (KN)
97	0.00	Dead+Live	9.80	5.46	0.80	5.67	5.54
138	0.00	Dead+Live	7.36	5.20	0.80	6.23	6.08

The lengths of the frames 97 and 138 (5.46m and 5.20m, respectively) caused the buckling capacity to fall short in the combination ‘Dead+Live’, as it is the most critical in downward loads and therefore the one that most compressed the elements. In the attempt of resolving this issue, the frames were strengthened by making it a three culm section, with a cross section as represented in the image below. This way, the value of the element’s crushing capacity $P_{\mathrm{c}} = f_{\mathrm{c}} \times \Sigma A$ (18) triples, increasing the value of the resistance, as well as transmitting a more robust appearance to the structure.

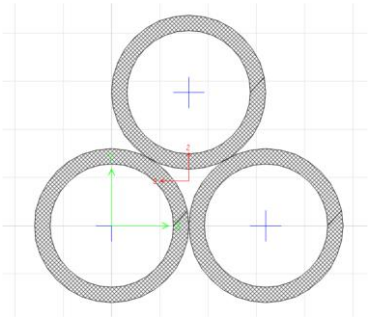

Figure 36- Cross section designed in SAP2000 for overstressed diagonals.

Although the cross section above was designed addressing symmetry concerns, it is important to remember that the inertia used to calculate the buckling capacity of these elements is still the inertia of a single culm, as required in (17). This means that although the culms are connected, it is considered that they would buckle as an individual culm. Even so, the design applied load distributed by the three culms is now inferior to the compressive capacity of each culm. All diagonals (illustrated below) were assigned this triple section.

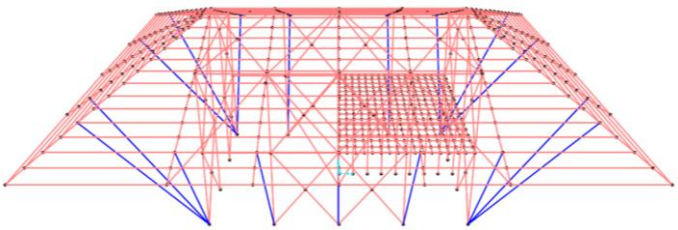

Figure 37- Elements with a strengthened section in blue.

Aside from the diagonals, solely one more element surpassed the compressive capacity in the most substantial wind load combination. The frame in question is illustrated in Figure 38 and the comparison of results are shown in Table 15. The values of stress differ for the symmetric frames since the loads vary along the roof and the rigidity added from the floor elements also results in an asymmetric stress distribution.

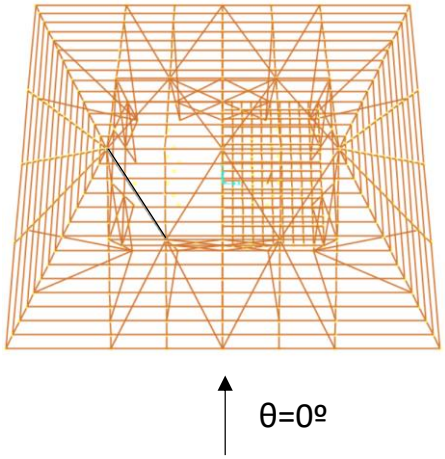

Figure 38- Highlight of the overstressed element.

Table 15- Summary of results of an element in the roofing structure.

Frame	Station	OutputCase	P (KN)	L (m)	Cbow	Pe (KN)	Ncr (KN)
310	3.74	COMB_0_1.5	12.50	3.74	0.80	12.06	11.44

Given the difficulty in varying the section of a single or very few elements of the roof in the construction process, a solution was found by decreasing the length between points of lateral restraint to half. This will consequently increase the buckling capacity from 12,06 kN to 48,25 kN, and the compressive capacity from 11,44 kN to 35,01 kN of the new couple of 1.87m long elements. To implement symmetry, the bracing elements of the final roofing structure are as illustrated in the figure below.

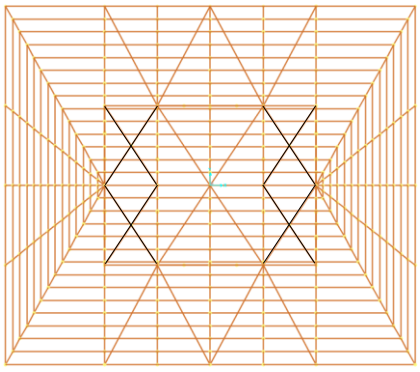

Figure 39- Alternative design of the roof structural elements.

After the modifications mentioned above (in the diagonal elements and in the roof structure), the remaining compressed frames all verify safety. The following most compressed elements, all present in the roof, are described below (frames 1543 and 21 are in the centreline of the figure).

Frame	Station	OutputCase	P (KN)	L (m)
1543	0.00	COMB_90_1.5	-28.76	2.00
21	0.00	COMB_90_1.5	-19.19	2.00
1171	0.00	COMB_90_1.5	-16.34	0.57
58	0.00	COMB_90_1.5	-16.18	0.57

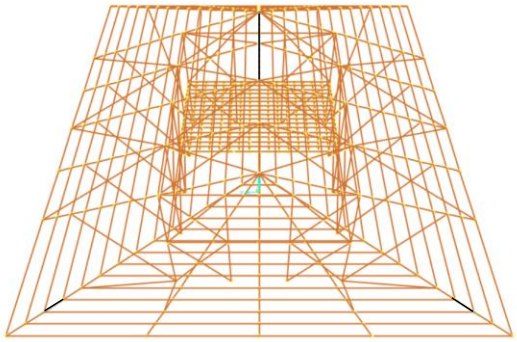

Figure 40- Characterization of the most compressed elements after modifications.

Buckling was the main and most evident cause of the safety verifications to fail. The results allow some awareness of the type of stress and element length that lead to excessive loads according to ISO 22156. Going deeper into this analysis, and to have a clearer idea of how these variables can compromise safety, the graphics below show the relation between L (length between points of lateral restraint) and buckling capacity (P_e), as well as L and the compressive capacity (N_{cr}).

Of course these values are only true for the assumptions taken specifically in this study. The variables in the function are E_{d}, I, C_{bow} and K, all described and quantified previously.

Note that the design value of 8.118 MPa was used for all the calculations. For wind and seismic loads, the load duration factor for modulus, C_{DE} equals to 1.0, which means that E_{c} is equal to 18,04 MPa for instantaneous loads. Even though this value was not considered in this study it is important to observe the differences. For the same lengths, the buckling and compressive capacity using E_{c} = 18,04 MPa corresponds to the lines “Pe 2” and “Ncr 2” (KN), respectively, in the graph below.

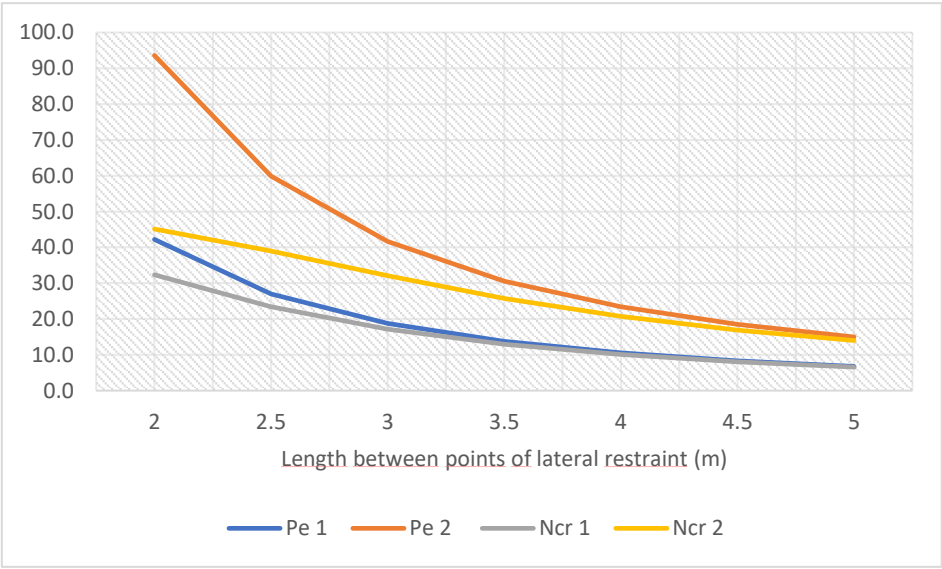

Figure 41- Relation between buckling and compressive capacity and length between points of lateral restraint for. E_{c} = 8.118 MPa and E_{c} = 18,04 MPa.

The results show an increase proportional to the increase of MOE in the 5 meter long elements, and quadratic increase as the length decreases. Elements over 5 m long will begin to show low resistances that will likely fail to verify safety if used as nun-redundant members.

The graphs below also help understand the variation of buckling and compressive capacity for different cross sections and consequently inertias. Four different outer diameters, wall thicknesses and inertias (described in Table 16) were considered, assuming E_c = 18,04 MPa and f_c =18,93 MPa.

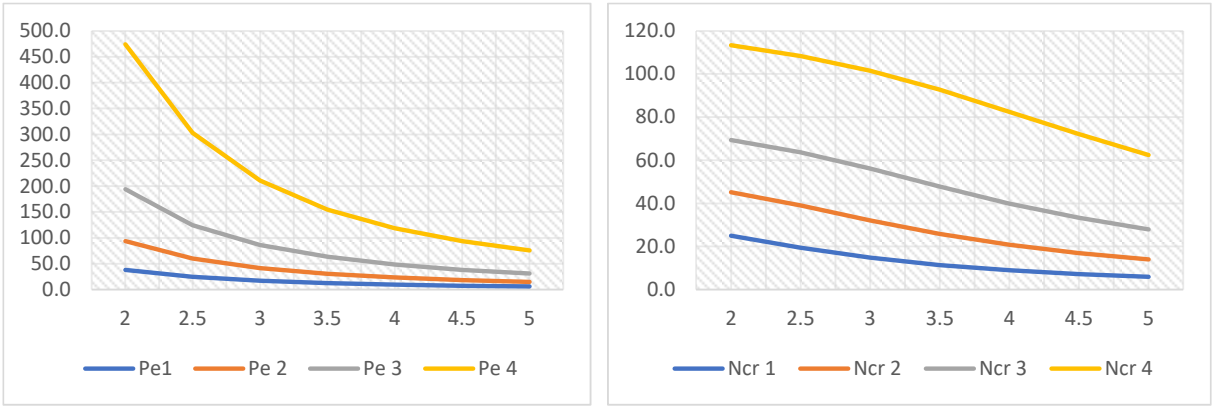

(a) (b)

Figure 42- Relation between buckling (a) and compressive (b) capacity and length between points of lateral restraint for four different culm geometries and taking E_c = 18,04 MPa and f_c =18.93 MPa.

Table 16- Characteristics of four generic culms used above.

	1	2	3	4
D (m)	0.08	0.10	0.12	0.15
δ (m)	0.008	0.010	0.012	0.015
I (m^4)	1.19E-06	2.90E-06	6.01E-06	1.47E-05
A (m^2)	1.81E-05	2.83E-05	4.07E-05	6.36E-05
fc (MPa)	34.25	53.52	77.07	120.43

The information demonstrates that especially for elements with an inferior length (but for all elements up to 5 meters of length), a larger cross section results in considerable enhancements in terms of buckling and compressive capacity, using the same compression strength parallel to fibres and MOE. Although in this particular study it was not the case, increasing the section of the poles used may enable structures to verify safety according to ISO 22156:2021.

5.7.2. Tension

For tension, the maximum value was still quite far from the tension capacity. The most tensioned frame is characterized below.

Frame	Station	OutputCase	P (KN)	Trd (KN)
953	1.41	COMB_90_1.5	21.65	238

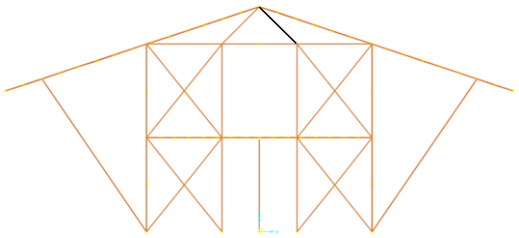

Figure 43- Characterization of the frame under the highest tension.

5.7.3. Bending

The resisting moment also demonstrated to be substantially higher than the applied moment. The frame with the highest flexural moment is characterized below.

Frame	Station	OutputCase	M2 (KN/m)	Mrd (KN)
1007	0.00	COMB_90_1.5	7.98	198

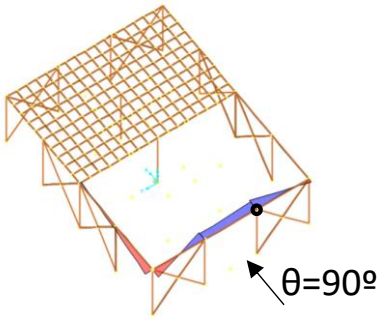

Figure 44- Characterization of the frame under the highest moment.

To avoid mechanisms, the horizontal frames in the figure were defined as continuous in the program and therefore are subjected to bending.

5.7.4. Combined Axial And Bending Loads

Given the difference between the results of bending moments applied and the moment capacity, this verification did not show critical frames in the structure. For tension combined with bending, the results were far from not verifying Equation (23. In the combination of compression and bending, the highest value of the Equation (22 came at 0,89. Interestingly, the frame in question has moments in both directions equal to zero, meaning that the value of the compression part of the equation had all of the accountability for the final result. The most consequential value is present on the roof structure, where the most compressed frame is present.

Table 17- Results for frame 1543.

Frame	Station	OutputCase	P (KN)	M2 (KN/m)	M3 (KN/m)	L (m)	Pe (KN)	Nrd (KN)	B
1543	0.50	COMB_90_1.5	-28.76	0.00	0.02	2.00	42.22	32.34	3.32

5.7.5. Deflections

The load combination “Service” defined in Table 6 was used to evaluate the deflections in the structure, as deflections occur under serviceability limit states. One of the reasons for including a floor was to understand how bamboo culms would behave as a flooring structural element. No significant stresses emerged in the flooring elements, yet they did need to suffer some alterations due to some large displacements.

The model was composed of continuous beams in the direction of smallest span (3m) and pinned in the perpendicular direction, unless for the centre beam (represented in black in Figure 45), that would end up having the columns under its length.

The live loads were once again introduced individually, multiplying the value recommended by the National Standard for floors (2kN/m^2) by the area of influence. The design reference for maximum allowable displacement was L/200 = 3/200 = 0,015 m or 1,5 cm.

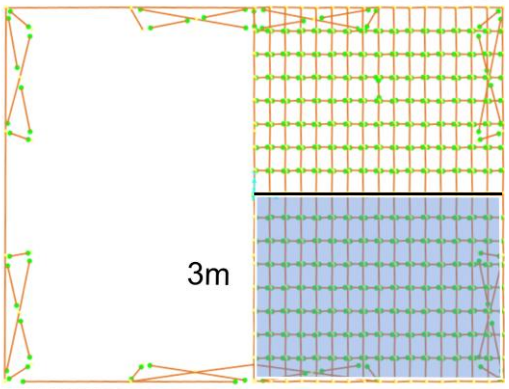

Figure 45- Representation of the structural elements of the floor.

Several iterations were done, beginning with decreasing the distance between continuous beams from 0.4m to 0.33m, reaching a final separation of 0.25m. In the perpendicular direction, the pinned culms were separated by 0.375m. To further decrease vertical displacements, a vertical element was inserted along the beam represented in black (Figure 46a), although the maximum displacement value would still come as 0.0285m. Finally, two more columns were introduced as in Figure 46b), which resulted in an acceptable maximum displacement of 0.0145m.

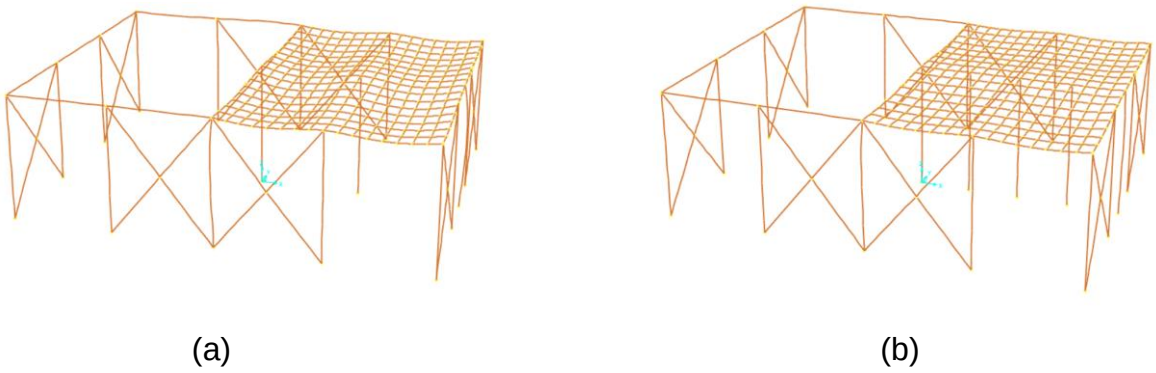

(a) (b)

Figure 46- a) Deflections resultant from service load combination with a single culm under the middle beam. b) With four culms supporting the middle beam.

These additional columns did not interfere with the architecture of the residence, as the area in blue in Figure 45 of the bottom floor, now separated by a wall along the black line from its 'twin' area, equals to a total of 12m^2. This is a very reasonable area for a bathroom and was thought to be one from the beginning of the design of the structure.

5.7.6. Shear

For shear loads, the values of resistance differ for permanent or instantaneous loads. After running all the load cases, there were no excesses of shear stress for permanent loads. For instantaneous loads, where the wind action is included, some irregularities appeared. In the roof, there were two specific elements with a shear load higher than the allowable, although this was caused by the model simplifications. This occurred when applying loads originated from the wind in the wall of the structure.

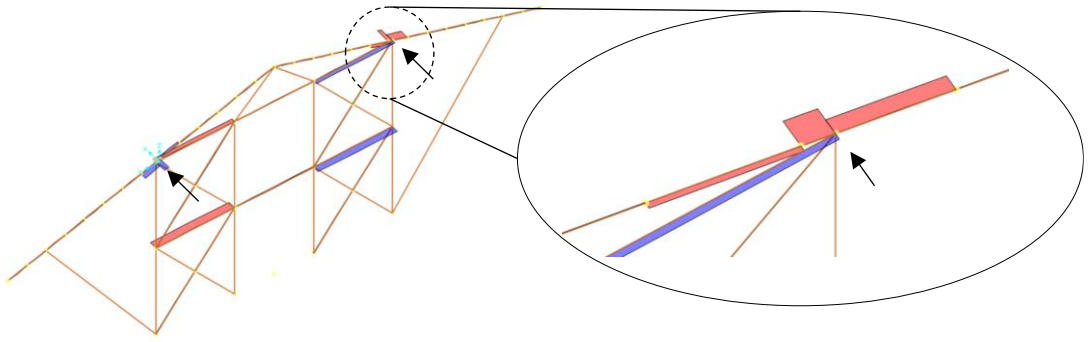

Figure 47- Detail of the overstressed frames for shear.

The figure above shows the elements in cause. The wind loads were applied individually in the nodes, which leads to a slightly different load path compared to having a wall transmitting the stresses to the frames. The overstressed element belongs to the roof diagonal, and the loads from the walls will mostly be transmitted to the bottom frame, as the roof element will be above the point in question.

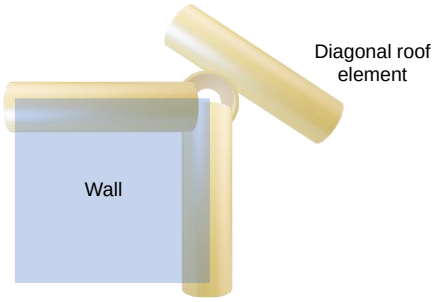

Figure 48- Detail of the elements in the frame corner.

For the stresses to be transferred between elements, the frames must be connected by a node. Therefore, a long continuous element is divided into a series of smaller continuous elements, so that the loads are transferred throughout its length. Also, the elements in the program are represented as lines in the mid section of the culm, which also makes the load transfers in the nodes slightly inaccurate when the nodes are closer than the diameter of the culm.

Accounting the alterations due to the deflections in the previous chapter, other excessive shear forces emerged in the central beam of the floor, due to the loads transferred to the columns below the element. The maximum shear force was 11,65 kN for the combination “COM_90_1.5” (described in Table 6), whereas the shear resistance for instantaneous loads determined previously is equal to 8,33 kN.

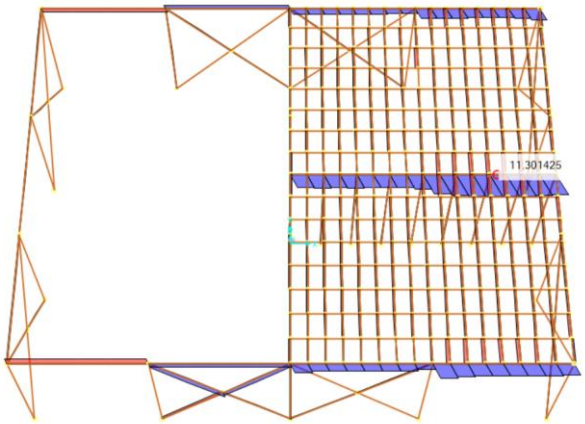

Figure 49- Demonstrations of the shear forces at the floor level (SAP2000).

To solve this, it is a possible solution to add another culm to the centre beam and to the columns that support it, decreasing the stress on each element, as illustrated in figure below.

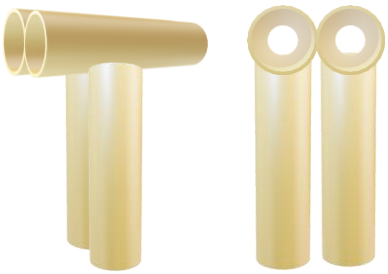

Figure 50- Illustration of a possible solution to avoid shear forces in the centre beam of the floor.

Besides these previous cases, all the remaining elements verified shear safety. The maximum values described and illustrated below were once again present in the roof.

Table 18- Characterization of the frames with the highest shear stresses.

Frame	Station	OutputCase	V2 (KN)
546	0.38	COMB_90_1.5	7.19
583	0.00	COMB_90_1.5	-7.25

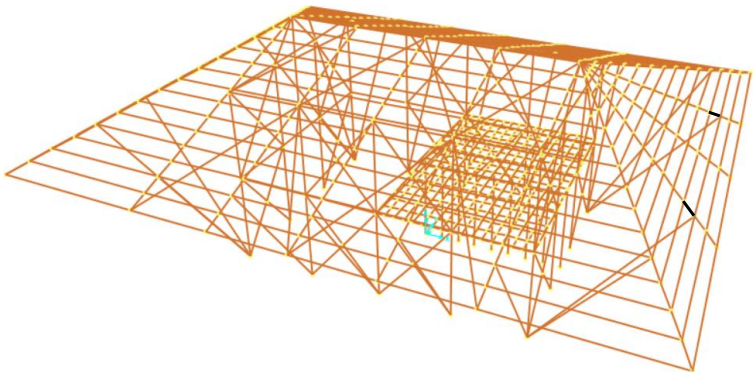

Figure 51- Elements 546 and 583 in black.

It was somewhat predictable that shear forces would be more substantial in these areas as the loads are transferred almost perpendicularly between the diagonals and the roof. Nevertheless, the shear forces were below the allowable value.

5.7.7. Dynamic Analysis

The seismic analysis was performed using the computer program SAP2000, as it has the option to run dynamic analysis considering the Eurocode (2004) and using the characteristics of the seismic action for Portugal, specifically.

The software analyses the structure through a modal analysis with multiple degrees of freedom, using the response spectra and the correspondent design peak ground accelerations. There are two types of earthquakes in Portugal (Type 1 and Type 2), distinguished by different surface wave magnitudes and geographic origins.

5.7.7.1. Design Ground Acceleration

To define the functions of the response spectrums, the value of the peak ground accelerations was taken from the Portuguese norm for Eurocode 8 (NP EN 1998-1, 2010). The figure below shows the different seismic zones (the zone considered is highlighted), and the following table the correspondent accelerations.

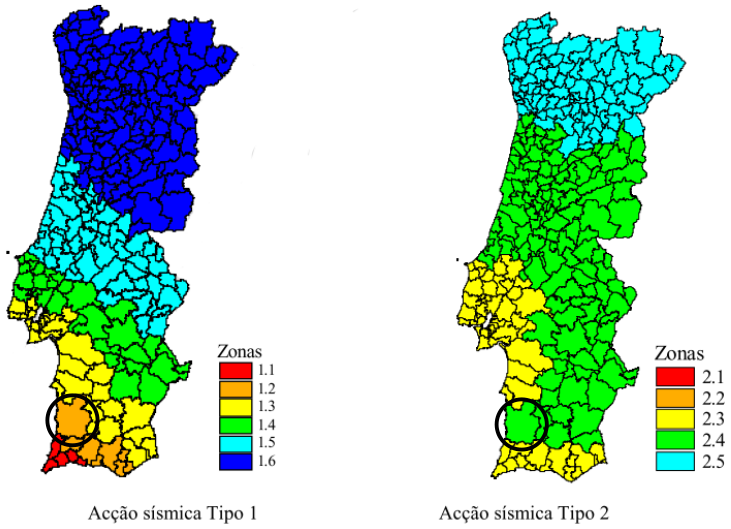

Figure 52- Seismic Zones for Type 1 (left) and Type 2 (right).

Table 19- Values of the reference peak ground acceleration a_{gR} for the seismic zone of the structure.

Type 1		Type 2	
Seismic Zone	agR (m/s^2)	Seismic Zone	agR (m/s^2)
1,2	2,0	2,4	1,1

Since the analysis is for a current structure (not as consequential as a school, hospital, etc.), the design ground acceleration is the same as the peak ground acceleration. Below are the parameters and illustration of the response spectrum for an earthquake Type 1 in a seismic zone 1.2.

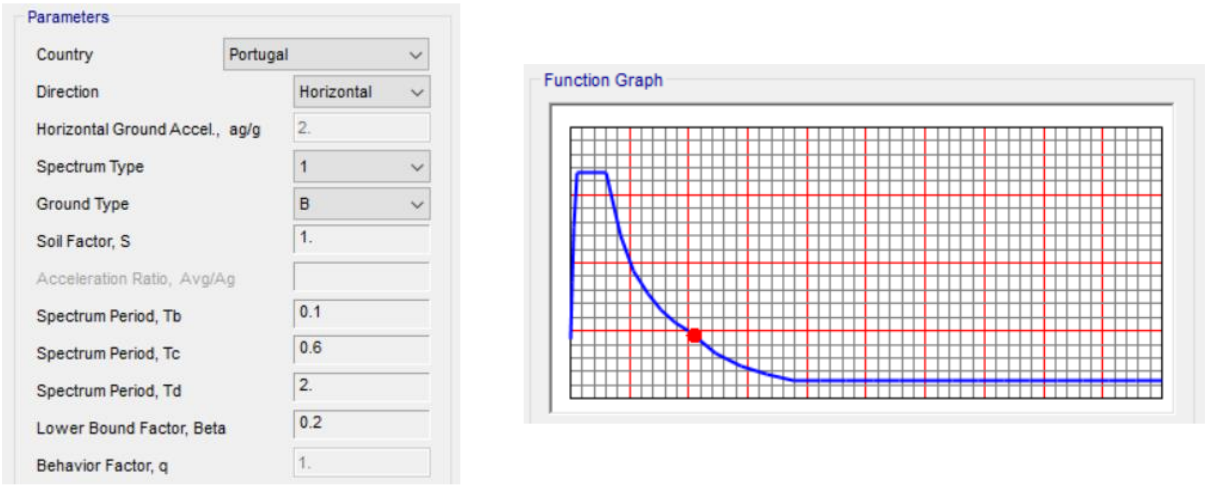

Figure 53- Response spectrum and parameters for an earthquake Type 1, seismic zone 1.2.

5.7.7.2. Load combinations

In the combinations for the seismic action, the vertical loads are defined by the European standard (NP EN 1998-1, 2010), using the expression below, which is also used to define the mass associated with the seismic movement of the structure.

$$\Sigma G_{k,j} + \Sigma \psi_{\mathrm{E,i}} \cdot Q_{\mathrm{k,i}} \tag{25}$$

with

$$\psi_{\mathrm{Ei}} = \varphi \cdot \psi_{2\mathrm{i}} \tag{26}$$

The value of ψ_2 defined in EN 1990:2002 is equal to 0,3 for domestic and residential areas, and φ is the highest for the roof ($\varphi = 1$), so that was the value used for the whole structure.

It is also important to acknowledge that the values returned from the software in terms of the internal forces are presented as absolute values. Meaning that for each direction, it is not disclosed if the resultant force is positive or negative, as it could be both. Therefore, the results from the seismic action must be both added and subtracted to the dead and live loads of (25, in both directions and for both of the earthquake types, resulting in eight combinations.

- $COMB\_T1\_X = 1{,}0 \times DeadLoad + \ 1{,}0 \times Steel\ Plate + 0{,}3 \times LiveLoad \ \pm Sismo\_1\_X$
- $COMB\_T2\_X = 1{,}0 \times DeadLoad + \ 1{,}0 \times Steel\ Plate + 0{,}3 \times LiveLoad \ \pm Sismo\_2\_X$

The combinations above are repeated for the Y direction.

By default, the software provides 12 modes when running the analysis. For this number of modes (equivalent to the number of degrees of freedom), the modal participating mass ratios in both directions demonstrated to be significantly low, and as a result, so would the internal forces. The first mode, for example, with the lowest frequency of 1.43 Hz moved approximately 0% of mass for each direction. Therefore, the number of modes was increased until the sum of modal participating mass ratios reached

90%, as recommended. For 75 modes, participation values came at 91,12% for Ux and 92,9% for Uy. This way, the stresses caused by the most consequential frequencies are guaranteed to be considered. The table below presents the characterization of the two modes that represent a higher participation ratio for Ux and Uy in the structure.

Table 20- Higher modal participating mass ratios of the structure.

Mode	UX	UY	Frequency (Hz)	Period (s)
22	0.39	1.3E-05	3.68	0.27
14	0.36	1.91E-06	3.00	0.33
21	1.89E-05	0.53	3.43	0.29
2	0.7E-03	0.26	2.14	0.47

5.7.7.3. Stress Analysis

The structure under analysis has the clear advantage of being extremely lightweight in comparison to what it would be if traditional construction materials were used. The global force in the z direction is equal to 32,78 kN, expressing the same idea. The values of the forces in the frames for the combinations mentioned above were far from exceeding the values of resistance in any type of stress, as Table 21 demonstrates.

Table 21- Results of the internal forces for seismic action.

	Frame	F	Resistance
Flexure (KN/m)	1168	-1.0993	197.88
Shear (KN)	693	5.339	8.33
Compression (KN)	39	-18.976	23.38
Tension (KN)	145	11.18	237.89

The only frame subjected to a force near its capacity was frame 39 illustrated in black below, under compression, characterized by a length of 2,5 m and a buckling capacity (P_e) equal to 27.02 kN.

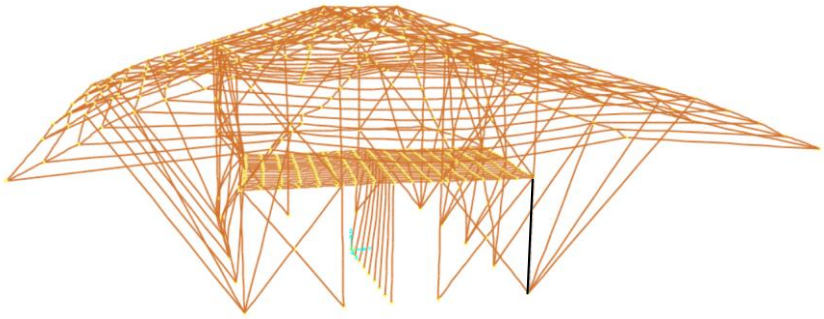

Figure 54- Deformed shape of the structure under seismic action.

Specified measures must be taken when designing the connections for the structures due to the brittle behaviour they may cause under seismic action. Nevertheless, the results of this dynamic analysis indicate that bamboo structures of this type are very capable of resisting earthquakes. Most of the frame forces computed by the software were far from reaching the allowable capacities calculated according to the new international structural design standard.

6. Conclusions and Future Developments

6.1. Conclusions

Bamboo is a functionally graded natural material that does not present uniform properties. Nevertheless, the variations are not particularly substantial and therefore do not compromise the structural safety of bamboo, if the right considerations are used.

Durability measures such as treatment with boron, seasoning, selecting mature bamboo and durability by design will protect the structure from beetles, termites, and rot. Consequently, the structure can last a lifetime (50+ years Kaminski et al. (2020)).

Regarding the connections, the number of tests performed is still considerably limited. The joints in bamboo are particularly challenging due to the nature of its cross section. This makes it hard to find reliable connections in the construction process, more than in other materials such as timber (Correal, 2019; Hong et al., 2019). However, there are several recent proposals that show efficacy in results. Radial clamping to resist splitting and improving ductility is a notable feature among the connections presented.

For an emerging anisotropic material as bamboo, the standards are largely responsible for enabling the confidence in using it as a reliable alternative, and a variety of thorough international standards are now available. Continuing the work on standardized testing, grading and structural design can make bamboo a conventional construction material.

The case study presents a static and dynamic analysis of a structure using bamboo as the only structural element. The response forces were obtained from the modelling computer program SAP2000 and compared with allowable resistances calculated according to the structural design standard ISO 22156:2021. The loads and combinations follow the Eurocode guidelines, as well as the documents for the country of Portugal. The project is defined to be implemented in the county of Odemira, as it is where the largest bamboo nursery in Europe resides (Viegas, n.d.). In it, grows the species Phyllostachys Edulis (Moso Bamboo) used in this study, one of the few species that has the majority of data on bamboo material properties. The bamboo culms were modelled as a linear elastic material and as hollow tubes with cross section dimensions characterized by an outer diameter of 0,1 m and a wall thickness of 0,01 m. All joints were assumed to be pinned.

The allowable strengths (f_i) were calculated using characteristic strength values (f_{ik}) from a study that tested 140 Moso bamboo culms from a supplier near São Paulo, Brazil (Gauss et al., 2020). These tests were performed according to testing standard ISO 22157-19 and defined as the 5th percentile value determined with 75% confidence, as required. The strength capacities for permanent and instantaneous loads resulted in the following:

Table 22- Maximum stress values of compression, tension, bending and shear. The stress values multiplied by the cross sectional area result in the values in kN.

fi	fik	Permanent		Instantaneous	
	MPa	MPa	kN	MPa	kN
fc (compression)	49.5	12.25	34.63	18.93	53.53
ft (tension)	220	54.45	153.93	84.15	237.89
fm (bending)	183	45.29	2.63	70.00	4.00
fv (shear)	15.4	1.91	5.39	2.95	8.33
MOE	18,040	8,118	-	18,040	-

Values of allowable resistance indicate great competence of bamboo as a structural element.

After running the analysis for the combinations including different dead, live and wind loads, the results showed that shear and bending were, as expected, the predominant concerns. Shear resistance is considerably low due to the tendency of longitudinal splitting of bamboo, and the buckling capacity of the culms compromises its compressive capacity. Therefore, modifications of the structure had to be implemented in order to obtain acceptable stresses. Columns holding the bamboo floor generated the most significant shear values in the beams, and the most compressed elements with higher length needed to be modified or supported.

In service conditions, the vertical displacements of the bamboo floor also led to some modifications in order to comply with the European reference of maximum allowable displacement L/200 = 3/200 = 0,015 m or 1,5 cm, in this case.

For the dynamic analysis, the software allows the configuration using the Eurocode (2004) and the characteristics of the seismic action for Portugal, specifically. The inputs in the program were the response spectra and correspondent design peak ground accelerations, characteristic of the two types of earthquakes that occur in Portugal and the seismic zone of the structure. The advantageously low self weight of bamboo (8 kN/m^3 or 815,77 kg/m^3 used in this study), resulted in a total weight of 32,78 kN. As a result, the forces caused by the seismic action were far from exceeding the values of allowable resistance for the combinations described in the European standard. The dynamic analysis results indicate that bamboo is exceedingly capable of resisting the earthquakes considered.

The study presented in this dissertation suggests that bamboo design has notable potential as a sustainable, durable, seismically resistant housing alternative, if cautions efforts in the design guarantee its safety and durability. Continuing the work on standardized testing, grading and structural design can make bamboo a conventional construction material.

6.2. Future Developments

Many aspects need further improvement in bamboo construction. The literature review indicates that the connections are perhaps the most underdeveloped element to consider. Testing new alternatives that compare weight, strength, ductility, cost, reliability, and durability is essential. This way, viable joint solutions will evolve from often being the most vulnerable part in bamboo structures (Kaminski,

Lawrence, & Trujillo, 2016). Efforts in development of joints capable of transmitting bending moment from beams to columns are also required to progress.

Durability treatments seem to have reached a fair level of confidence, yet the demonstration of long term results have not yet been densely provided. It is also relevant to contribute with new ways to implement the protection and safety of bamboo in architecture and construction.

Curved arcs made of many bamboo splits or smaller diameter culms seem to have been growing in recent implemented projects around the world. Standardized measurements of the resistance of these elements will improve the knowledge in structural design alternatives using bamboo.

In regard to testing, the increase of documents pointing the material properties of different species of bamboo growing around the world is essential for reasonable design. The present study would have ideally used values from mechanical tests of Moso bamboo that had grown in Portugal.

In the case study, a deeper analysis of the variation of the cross section can be further developed, as well as the study of different characteristic strength values natural from different species.

Providing a connection design safely applicable in the structure and a thorough final project would also be relevant for academics developing bamboo housing alternatives. Moreover, different structure geometries would also help understand how bamboo's properties can be optimized, without compromising durability by design measures. Real scale earthquake testing of the structures developed would produce more relevant data on the seismic analysis.

References

Abdul Latif, M., Wan, T., Fauzidah, A., 1990. Anatomical features and mechanical properties of three Malaysian bamboos*. J. Trop. For. Sci. 2 (3),* 227e334. Quoted in D. J. Trujillo & López (2019).

Amada, S., Munekata, T., Nagase, Y., Ichikawa, Y., Kirigai, A., & Zhifei, Y. (1996). The mechanical structures of bamboos in viewpoint of functionally gradient and composite materials. *Journal of Composite Materials*, *30*(7), 800–819. https://doi.org/10.1177/002199839603000703

Anokye, R., Kalong, R. M., Bakar, E. S., Ratnasingam, J., Jawaid, M., & Awang, K. (2014). Variations in moisture content affect the shrinkage of Gigantochloa scortechinii and Bambusa vulgaris at different heights of the Bamboo Culm. *BioResources*, *9*(4), 7484–7493. https://doi.org/10.15376/biores.9.4.7484-7493

Asif, M. (2009). Sustainability of timber, wood and bamboo in construction. In *Sustainability of Construction Materials*. Woodhead Publishing Limited. https://doi.org/10.1533/9781845695842.31

Asociación colombiana de ingeniería sismica (AIS). (2010). NSR-10 Título G-Estructuras de madera y estructuras de guadua. *Ministerio de Ambiente, Vivienda y Desarrollo Territorial*, 158.

Awaludin, A., & Andriani, V. (2014). Bolted bamboo joints reinforced with fibers. *Procedia Engineering*, *95*(Scescm), 15–21. https://doi.org/10.1016/j.proeng.2014.12.160

Bamboo U. (2021). Bamboo Architecture Design and Construction Course. https://bamboou.com/

Banik, R. L. (2015). *Morphology and Growth*. Springer International Publishing Switzerland 2015 W. https://doi.org/10.1007/978-3-319-14133-6_3

Berndsen, R. S. (2008). *Caracterização Anatômica, Física e Mecânica de Lâminas de Bambu (Phyllostachys pubescens)*.

Correal D., J. F., & Arbeláez C., J. (2010). Influence of age and height position on colombian Guadua angustifolia bambo mechanical properties. *Maderas: Ciencia y Tecnologia*, *12*(2), 105–113. https://doi.org/10.4067/S0718-221X2010000200005

Correal, F. (2019). Bamboo design and construction. In *Nonconventional and Vernacular Construction Materials: Characterisation, Properties and Applications*. Elsevier Ltd. https://doi.org/10.1016/B978-0-08-102704-2.00019-6

Correal, J. F., & Echeverry, J. S. (2015). Dowel-Bearing Strength Behaviour of Guadua angustifolia Kunth Bamboo. *Proceedings of 16th NOCMAT Conference*.

CSI Portugal | SAP2000. (n.d.). Retrieved October 24, 2021, from https://www.csiportugal.com/software/2/sap2000

Deng, J., Chen, F., Wang, G., & Zhang, W. (2016). Variation of Parallel-to-Grain Compression and Shearing Properties in Moso Bamboo Culm (Phyllostachys pubescens). *BioResources*, *11*(1), 1784–1795. https://doi.org/10.15376/biores.11.1.1784-1795

Dixon, P. G., Ahvenainen, P., Aijazi, A. N., Chen, S. H., Lin, S., Augusciak, P. K., Borrega, M., Svedström, K., & Gibson, L. J. (2015). Comparison of the structure and flexural properties of Moso, Guadua and Tre Gai bamboo. *Construction and Building Materials*, *90*, 11–17. https://doi.org/10.1016/j.conbuildmat.2015.04.042

Dixon, P. G., & Gibson, L. J. (2014). The structure and mechanics of Moso bamboo material. *Journal of the Royal Society Interface*, *11*(99). https://doi.org/10.1098/rsif.2014.0321

EN 1990:2002. (n.d.). *1*(2005).

Environmental Bamboo Foundation. (n.d.). Environmental Bamboo Foundation | Working on Rural Community Empowerment, Landscape Restoration, and Sustainable Forestry in Indonesia. Retrieved October 22, 2021, from https://www.bambuvillage.org/

Eurocode 1: Wind actions. (2005). *Actions on*(5), 18-22+95. https://doi.org/10.4324/9781315780320-29

Fu, Y., Shao, B., & Fu, S. (2013). Comparative Study of Mechanical Performance of Bamboo Joints. *Advances in Structural Engineering and Mechanics*, 2446–2456.

Galeria de Templo Luum / CO-LAB Design Office - 5. (n.d.). Retrieved June 17, 2021, from https://www.archdaily.com.br/br/921542/templo-luum-co-lab-design-office/5d04123c284dd13726000066-luum-temple-co-lab-design-office-image?next_project=no

Gauss, C., Harries, K. A., Kadivar, M., Akinbade, Y., & Savastano, H. (2020). Quality assessment and mechanical characterization of preservative-treated Moso bamboo (P. edulis). *European Journal of Wood and Wood Products*, *78*(2), 257–270. https://doi.org/10.1007/s00107-020-01508-x

Gauss, C., Savastano, H., & Harries, K. A. (2019). Use of ISO 22157 mechanical test methods and the characterisation of Brazilian P. edulis bamboo. *Construction and Building Materials*, *228*,

116728. https://doi.org/10.1016/j.conbuildmat.2019.116728
Godina, M., & Lorenzo, R. (2015). Calibrating a composite material model for analysis and design of bamboo structures. *10th World Bamboo Congress*. http://www.worldbamboo.net/wbcx/Sessions/Theme Architecture Engineering Social Housing/Godina, Martha Lorenzo, Rodolfo .pdf
Grand View Research. (n.d.). Bamboos Market Size & Share | Global Industry Report, 2019-2025. Retrieved October 22, 2021, from https://www.grandviewresearch.com/industry-analysis/bamboos-market
Habibi, M. K., Samaei, A. T., Gheshlaghi, B., Lu, J., & Lu, Y. (2015). Asymmetric flexural behavior from bamboo's functionally graded hierarchical structure: Underlying mechanisms. *Acta Biomaterialia*, *16*(1), 178–186. https://doi.org/10.1016/j.actbio.2015.01.038
Hallwood, A. J., and Horrobin, S. (1946). "Absorption of water by polymers: Analysis in terms of a simple model," *Transactions of the Faraday Society* 42B, 84-102. Quoted in Jiang et al. (2012).
Harries, K. A., Bumstead, J., Richard, M., & Trujillo, D. (2017). Geometric and material effects on bamboo buckling behaviour. *Proceedings of the Institution of Civil Engineers: Structures and Buildings*, *170*(4), 236–249. https://doi.org/10.1680/jstbu.16.00018
Harries, K. A., & Sharma, B. (2020). Nonconventional and Vernacular Construction Materials. In *Nonconventional and Vernacular Construction Materials*. https://doi.org/10.1016/c2017-0-04244-1
Harries, K. A., Sharma, B., & Richard, M. (2012). Structural Use of Full Culm Bamboo: The Path to Standardization. *International Journal of Architecture, Engineering and Construction*, *1*(2), 66–75. https://doi.org/10.7492/ijaec.2012.008
Hodgkin, D. (2009). Humanitarian Bamboo - A manual on the humanitarian use of bamboo in Indonesia. In *Manual*. https://es.scribd.com/document/21153630/Humanitarian-Bamboo-a-manual-on-the-humanitarian-use-of-bamboo-in-Indonesia
Hong, C., Li, H., Lorenzo, R., Wu, G., Corbi, I., Corbi, O., Xiong, Z., Yang, D., & Zhang, H. (2019). Review on connections for original bamboo structures. *Journal of Renewable Materials*, *7*(8), 714–730. https://doi.org/10.32604/jrm.2019.07647
INBAR. (2020). *Transfer of Technology Model: Village Bamboo Preservation Unit*.
InCide Technologies. (2013). *Material Safety Data Sheet BOARD DEFENSE (Insecticide, Termiticide and Fungicide) SECTION 1 -CHEMICAL PRODUCT AND COMPANY IDENTIFICATION*.
International Bamboo and Rattan Organisation. (2021). Bamboo and Rattan Update. *INBAR Magazine*, *2*(1), 1–20. www.inbar.int/bru-magazine/
ISO. (2004a). *ISO/TR 22157-2:2004 - Bamboo — Determination of physical and mechanical properties — Part 2: Laboratory manual*. https://www.iso.org/standard/38360.html
ISO. (2004b). *ISO 22156:2004 - Bamboo — Structural design*. https://www.iso.org/standard/36149.html
ISO. (2004c). *ISO 22157-1:2004 - Bamboo — Determination of physical and mechanical properties — Part 1: Requirements*. https://www.iso.org/standard/36150.html
ISO. (2018). *ISO 19624:2018 - Bamboo structures — Grading of bamboo culms — Basic principles and procedures*. https://www.iso.org/standard/65528.html
ISO. (2019). *ISO 22157:2019 - Bamboo structures — Determination of physical and mechanical properties of bamboo culms — Test methods*. https://www.iso.org/standard/65950.html
ISO 22156:2021. (2021). *INTERNATIO*.
Janssen, J.J., 2000. Designing and Building with Bamboo*. INBAR Technical Report No. 20. International Network for Bamboo and Rattan (INBAR), Beijing*. Quoted in F. Correal (2019).
Jiang, Z., Wang, H., Tian, G., Liu, X., & Yu, Y. (2012). Properties of Moso Bamboo To Moisture Content. *BioResources*, *7*, 5048–5058.
Kaminski, S. (2013). *Engineered bamboo houses for low-income communities in Latin America - The Institution of Structural Engineers*. *april 2016*. https://www.istructe.org/journal/volumes/volume-91-(2013)/issue-10/engineered-bamboo-houses-for-low-income-communitie/
Kaminski, S. (2018). *Rohingya Refugee Camps and Sites , Cox ' s Bazar Region , Bangladesh*. *November*.
Kaminski, S., Harries, K. A., & Trujillo, D. (2020). *Webinar | Structural use of bamboo culms (Part 1)*. YouTube. https://www.youtube.com/watch?v=hk_484Hx060&t=4549s
Kaminski, S., Laurence, A., & Trujillo, D. (2016). Structural use of bamboo. : Part 1: Introduction to bamboo. *Structural Engineer*, *94*(8).

Kaminski, S., Lawrence, A., & Trujillo, D. (2016). *Design Guide for Engineered Baharaque Housing*.
Kaminski, S., Lawrence, A., Trujillo, D., & King, C. (2016). Structural use of bamboo Part 2 : Durability and Preservation. *Structural Engineer*, *94*(10), 38–43.
Lefevre, B., West, R., O'Reilly, P., & Taylor, D. (2019). A new method for joining bamboo culms. *Engineering Structures*, *190*(April), 1–8. https://doi.org/10.1016/j.engstruct.2019.04.003
Li, W.-T., Long, Y.-L., Huang, J., & Lin, Y. (2017). Axial load behavior of structural bamboo filled with concrete and cement mortar. *Construction and Building Materials*, *148*, 273–287. https://doi.org/10.1016/j.conbuildmat.2017.05.061
Li, X. B., Shupe, T. F., Peter, G. F., Hse, C. Y., & Eberhardt, T. L. (2007). Chemical Changes With Maturation of the Bamboo. *Journal of Tropical Forest Science*, *19*(1), 6–12.
Liese, W., 1998. The anatomy of bamboo culms. *INBAR Technical Report 18 International Network for Bamboo and Rattan - INBAR, Beijing, P.R. China.* Quoted in Harries & Sharma (2020).
Liese, W., 1985. Bamboos e Biology, Silvics, Properties, Utilization. *Deustche Gesellschaft Technische Zusammenarbeit (GTZ), GmbH*. Quoted in Harries & Sharma (2020).
Liese, W., Gutiérrez, J. & González, G. (2002) Preservation of bamboo for the construction of houses for low income people. *In: Bamboo for Sustainable Development,* pp. 481-494. Quoted in Kaminski (2018)
Liese, Walter. (2015). Bamboo: The plant and its uses. In *Bamboo: The plant and its uses*.
Liese, Walter, & Tang, T. K. H. (2015). *Preservation and Drying of Bamboo*. https://doi.org/10.1007/978-3-319-14133-6_9
Lo, T. Y., Cui, H. Z., & Leung, H. C. (2004). The effect of fiber density on strength capacity of bamboo. *Materials Letters*, *58*(21), 2595–2598. https://doi.org/10.1016/j.matlet.2004.03.029
Lu, X., Wang, K., Yi, X., Liou, J., He, J., 1985. A study on the physic-mechanical properties of culmwood of Phyllostachys Glauca of Shandong. *Zhejiang Forestry Science Research Institute, Hangzhou, China J. Bamboo* Res. 4 (2), 98-106. Quoted in Harries & Sharma (2020).
Lombok Bamboo Housing | Ramboll | Archello. (n.d.). Retrieved October 4, 2021, from https://archello.com/project/lombok-bamboo-housing
Lorenzo, R., Godina, M., Mimendi, L., & Li, H. (2020). Determination of the physical and mechanical properties of moso, guadua and oldhamii bamboo assisted by robotic fabrication. *Journal of Wood Science*, *66*(1). https://doi.org/10.1186/s10086-020-01869-0
Mendes, P. M., & Oliveira Pedro, J. J. (2020). *Dimensionamento de Estruturas de Edifícios e Estruturas Especiais*. IST Press.
Mitch, D., Harries, K. A., & Sharma, B. (2010). Characterization of Splitting Behavior of Bamboo Culms. *Journal of Materials in Civil Engineering*, *22*(11), 1195–1199. https://doi.org/10.1061/(asce)mt.1943-5533.0000120
Moran, R., & Silva, H. (2016). *Design of steel connectors for structural bamboo members*. *October*.
Moran, R., & Silva, H. (2017). A Bamboo Beam-Colum Connection Capable to Transmit Moment. *Non-Conventional Materials and Technologies*, *7*(December), 35–44. https://doi.org/10.21741/9781945291838-5
Nogata, F., & Takahashi, H. (1995). Intelligent functionally graded material: Bamboo. *Composites Engineering*, *5*(7), 743–751. https://doi.org/10.1016/0961-9526(95)00037-N
NP EN 1991-1-1. (2009). *Norma Portuguesa - Eurocódigo 1 : Ações em Estruturas - Parte 1-1: Ações Gerais*. *Eurocódigo*, 44.
NP EN 1998-1. (2010). *Instituto Português Da Qualidade*, *Eurocódigo*.
O FELIZ. (n.d.). Retrieved October 14, 2021, from https://www.ofeliz.pt/pt/downloads
Ota, M., 1953. Studies on the Properties of Bamboo Stem (Part 9*). On the Relation between Compressive Strength Parallel to Grain and Moisture Content of Bamboo Splint, vol. 22. Bulletin of Kyushu University of Forestry,* pp. 87e108. Quoted in Janssen (1991).
Ota, M., 1950. Studies on the properties of bamboo stem (part 7). *The influence of the per- centage of structural elements on the specific gravity and compressive strength of bamboo splint. Bull. Kyushu Univ. Forest. 19, 25e47.* Quoted in Janssen (1991).
Paraskeva, T., Pradhan, N. P. N., Stoura, C. D., & Dimitrakopoulos, E. G. (2019). Monotonic loading testing and characterization of new multi-full-culm bamboo to steel connections. *Construction and Building Materials*, *201*, 473–483. https://doi.org/10.1016/j.conbuildmat.2018.12.198
Rabik, A., & Brown, B. (2004). *TOWARDS RESILIENT BAMBOO FORESTRY A Reference Guide for Improved Management of Clumping*. 1–307.
Richard, M. J. (2013). Assessing the Performance of Bamboo Structural Components. *Journal of Chemical Information and Modeling*, *53*(9), 287.

Richard, M. J., & Harries, K. A. (2015). On inherent bending in tension tests of bamboo. *Wood Science and Technology*, *49*(1), 99–119. https://doi.org/10.1007/s00226-014-0681-9
Sánchez Cruz, M. L., & Morales, L. Y. (2019). Influence of moisture content on the mechanical properties of Guadua Culms. *Inge Cuc*, *15*(1), 99–108. https://doi.org/10.17981/ingecuc.15.1.2019.09
Sassu, M., De Falco, A., Giresini, L., & Puppio, M. L. (2016). Structural solutions for low-cost bamboo frames: Experimental tests and constructive assessments. *Materials*, *9*(5). https://doi.org/10.3390/ma9050346
Shao, Z. P., Zhou, L., Liu, Y. M., Wu, Z. M., & Arnaud, C. (2010). Differences in structure and strength between internode and node sections of moso bamboo. *Journal of Tropical Forest Science*, *22*(2), 133–138.
Shao, Zhuo Ping, Fang, C. H., Huang, S. X., & Tian, G. L. (2010). Tensile properties of Moso bamboo (Phyllostachys pubescens) and its components with respect to its fiber-reinforced composite structure. *Wood Science and Technology*, *44*(4), 655–666. https://doi.org/10.1007/s00226-009-0290-1
Sekhar, A.C., Rawat, B.S., Bhartari, R.K., 1962. *Strength of bamboos: Bambusa nutans. Indian For*. 67e73. Quoted in Janssen (1991).
Shu, J., & Wang, H. (2015). *Pests and Diseases of Bamboos*. 175–192. https://doi.org/10.1007/978-3-319-14133-6_6
Tang, T. K. H., Welling, J., & Liese, W. (2013). Kiln drying for bamboo culm parts of the species Bambusa stenostachya, Dendrocalamus asper and Thyrsostachys siamensis. *Journal of the Indian Academy of Wood Science*, *10*(1), 26–31. https://doi.org/10.1007/s13196-013-0089-4
Titilayo Akinlabi, E., Anane-Fenin, K., & Akwada, D. R. (2017). *Bamboo: The Multipurpose Plant*. Springer.
Trujillo, D. J. A., & Malkowska, D. (2018). Empirically derived connection design properties for Guadua bamboo. *Construction and Building Materials*, *163*, 9–20. https://doi.org/10.1016/j.conbuildmat.2017.12.065
Trujillo, D. J., & López, L. F. (2019). Bamboo material characterisation. *Nonconventional and Vernacular Construction Materials: Characterisation, Properties and Applications*, *2004*, 491–520. https://doi.org/10.1016/B978-0-08-102704-2.00018-4
Trujillo, D., & Jangra, S. (2016). *Grading of Bamboo* (Issue October 2016).
Trujillo, D., Jangra, S., & Gibson, J. M. (2017). Flexural properties as a basis for bamboo strength grading. *Proceedings of the Institution of Civil Engineers: Structures and Buildings*, *170*(4), 284–294. https://doi.org/10.1680/jstbu.16.00084
Viegas, H. (n.d.). *O maior viveiro de bambus da Europa está no Alentejo*. Noticiasmagazine. Retrieved October 20, 2021, from https://www.noticiasmagazine.pt/2017/alentejo-bambus-europa/historias/120171/
Wakchaure, M. R., & Kute, S. Y. (2012). Effect of moisture content on physical and mechanical properties of bamboo. *Asian Journal of Civil Engineering*, *13*(6), 753–763.
Wang, X., Cheng, D., Huang, X., Song, L., Gu, W., Liang, X., Li, Y., & Xu, B. (2020). Effect of high-temperature saturated steam treatment on the physical, chemical, and mechanical properties of moso bamboo. *Journal of Wood Science*, *66*(1). https://doi.org/10.1186/s10086-020-01899-8
Wang, X., Song, L., Cheng, D., Liang, X., & Xu, B. (2019). Effects of saturated steam pretreatment on the drying quality of moso bamboo culms. *European Journal of Wood and Wood Products*, *77*(5), 949–951. https://doi.org/10.1007/s00107-019-01421-y
Widyowijatnoko, A., & Harries, K. A. (2019). Joints in bamboo construction. In *Nonconventional and Vernacular Construction Materials: Characterisation, Properties and Applications*. Elsevier Ltd. https://doi.org/10.1016/B978-0-08-102704-2.00020-2
Widyowijatnoko, A., 2012. Traditional and Innovative Joints in Bamboo Construction (Ph.D. thesis). *RWTH Aachen University*. Quoted in Widyowijatnoko & Harries (2019).
World Green Building Council. (n.d.). Embodied Carbon Call to Action Report. Retrieved October 22, 2021, from https://www.worldgbc.org/embodied-carbon
Zhou, F., 1981. Studies on physical and mechanical properties of bamboo wood. *Journal of Nanjing Technical College, Forestry Products (2), 1-32. Quoted in Harries & Sharma (2020).*
L.A. Soltis, European yield model for wood connections*, in: Proc. Struct. Congr., American Society of Civil Engineers, Indianapolis, New York, 1991*, pp. 60–63. Quoted in Paraskeva et al. (2019).
ASTM, D7264 (2015) Standard test method for flexural properties of polymer matrix composite materials. *American Society for Testing and Materials, West Conshohocken*. Quoted in (Gauss

et al., 2020)

Annex

A 1-Protruding roof loads.

COMB θ=0º EXTERNAL					
LEEWARD L=15.5					
	LOAD	DL		CL	
		A (m2)	R (kN)	A (m2)	R (kN)
1	-0.55	1.838	-1.0109	1.016	-0.5588
2		1.702	-0.9361	1.016	-0.5588
3		1.566	-0.8613	1.016	-0.5588
4		1.429	-0.78595	1.016	-0.5588
5		1.293	-0.71115	1.016	-0.5588
6		1.157	-0.63635	1.016	-0.5588
7		1.021	-0.56155	1.016	-0.5588
8		0.885	-0.48675	1.016	-0.5588
9		0.749	-0.41195	1.016	-0.5588
10		0.613	-0.33715	1.016	-0.5588
11		0.476	-0.2618	1.016	-0.5588
12		0.34	-0.187	1.016	-0.5588
13		0.204	-0.1122	1.016	-0.5588
14		0.068	-0.0374	1.016	-0.5588

COMB θ=90º EXTERNAL					
LEEWARD L=13.5					
	LOAD	DL		CL	
		A (m2)	R (kN)	A (m2)	R (kN)
1	-0.55	1.13	-0.6215	0.904	-0.4972
2		1.016	-0.5588	0.837	-0.46035
3		0.962	-0.5291	0.77	-0.4235
4		0.879	-0.48345	0.703	-0.38665
5		0.795	-0.43725	0.636	-0.3498
6		0.711	-0.39105	0.569	-0.31295
7		0.628	-0.3454	0.502	-0.2761
8		0.544	-0.2992	0.435	-0.23925
9		0.46	-0.253	0.368	-0.2024
10		0.377	-0.20735	0.301	-0.16555
11		0.293	-0.16115	0.234	-0.1287
12		0.209	-0.11495	0.167	-0.09185
13		0.126	-0.0693	0.1	-0.055
14		0.042	-0.0231	0.033	-0.01815

A 2- External load verification for θ=0º.

EXTERNAL LOADS FOR 18º (KN/m2) for θ=0º									
	F	G	H	I	J	K	L	M	Σ
Area	5.105	12.197	61.196	44.724	13.341	12.197	8.2	21.319	226.244
X	2	1	1	1	2	1	2	2	
=	10.21	12.197	61.196	44.724	26.682	12.197	16.4	42.638	
cpi	-0.63271	-0.57098	-0.21605	-0.37037	-0.7253	-0.8179	-1.08024	-0.49382	-
Resultant	-6.45999	-6.96429	-13.2213	-16.5643	-19.3526	-9.97588	-17.7159	-21.0557	-111.31

A 3- External load verification for θ=90º.

EXTERNAL LOADS FOR 18º (KN/m2) for θ=90º								
	F	G	H	I	J	L	N	Σ
Area	3.138	5.02	18.224	13.12	8.2	13.341	70.262	226.246
x	2	1	1	1	2	2	2	
=	6.276	5.02	18.224	13.12	16.4	26.682	140.524	
cpe	-0.63271	-0.57098	-0.21605	-0.37037	-0.7253	-1.08024	-0.21605	-
Resultant	-3.9709	-2.86634	-3.93726	-4.85923	-11.895	-28.823	-30.3599	-86.7116

A 4- Reactions of external pressures for θ=0º.

	COMB θ=0º EXTERNAL												
	WINDWARD L=15.5						LEEWARD L=15.5						
	DW			CW				DL			CL		
	A (m2)	LOAD	cpe (kN)	A (m2)	LOAD	cpe (kN)		A (m2)	LOAD	cpe (kN)	A (m2)	LOAD	cpe (kN)
1	1.838	F	-0.58146	1.016	G	-0.29006	1	1.838	J	-0.66655	1.016	K	-0.41549
2	1.702	F	-0.53844	1.016	G	-0.29006	2	1.702	J	-0.61723	1.016	K	-0.41549
3	1.566	F	-0.49541	1.016	G	-0.29006	3	1.566	J	-0.56791	1.016	K	-0.41549
4	1.429	H	-0.15437	1.016	H	-0.10975	4	1.429	J	-0.51823	1.016	I	-0.18815
5	1.293	H	-0.13968	1.016	H	-0.10975	5	1.293	J	-0.46891	1.016	I	-0.18815
6	1.157	H	-0.12498	1.016	H	-0.10975	6	1.157	J	-0.41959	1.016	I	-0.18815
7	1.021	H	-0.11029	1.016	H	-0.10975	7	1.021	J	-0.37027	1.016	I	-0.18815
8	0.885	H	-0.0956	1.016	H	-0.10975	8	0.885	J	-0.32095	1.016	I	-0.18815
9	0.749	H	-0.08091	1.016	H	-0.10975	9	0.749	J	-0.27163	1.016	I	-0.18815
10	0.613	H	-0.06622	1.016	H	-0.10975	10	0.613	J	-0.22231	1.016	I	-0.18815
11	0.476	H	-0.05142	1.016	H	-0.10975	11	0.476	J	-0.17262	1.016	I	-0.18815
12	0.34	H	-0.03673	1.016	H	-0.10975	12	0.34	J	-0.1233	1.016	I	-0.18815
13	0.204	H	-0.02204	1.016	H	-0.10975	13	0.204	J	-0.07398	1.016	I	-0.18815
14	0.068	H	-0.00735	1.016	H	-0.10975	14	0.068	J	-0.02466	1.016	I	-0.18815

A 5- Reactions of external pressures for θ=0º.

	SIDE PARALEL TO WIND ACTION (L=13.5)							
	D1			D2		C		
	A (m2)	LOAD	cpe (kN)	LOAD	cpe (kN)	A (m2)	LOAD	cpe (kN)
1	1.13	L	-0.61034	M	-0.27901	0.904	M	-0.22321
2	1.046	L	-0.56497	M	-0.25827	0.837	M	-0.20667
3	0.962	L	-0.5196	M	-0.23753	0.77	M	-0.19012
4	0.879	L	-0.47477	M	-0.21704	0.703	M	-0.17358
5	0.795	L	-0.4294	M	-0.1963	0.636	M	-0.15704
6	0.711	L	-0.38403	M	-0.17555	0.569	M	-0.14049
7	0.628	L	-0.3392	M	-0.15506	0.502	M	-0.12395
8	0.544	L	-0.29383	M	-0.13432	0.435	M	-0.10741
9	0.46	L	-0.24846	M	-0.11358	0.368	M	-0.09086
10	0.377	L	-0.20363	M	-0.09309	0.301	M	-0.07432
11	0.293	L	-0.15826	M	-0.07235	0.234	M	-0.05778
12	0.209	L	-0.11289	M	-0.0516	0.167	M	-0.04123
13	0.126	L	-0.06806	M	-0.03111	0.1	M	-0.02469
14	0.042	L	-0.02269	M	-0.01037	0.033	M	-0.00815

A 6- Reactions of external pressures for θ=90º.

	COMB θ=90º EXTERNAL												
	WINDWARD L=13.5						LEEWARD L=13.5						
	DW			CW				DL			CL		
	A (m2)	LOAD	cpe (kN)	A (m2)	LOAD	cpe (kN)		A (m2)	LOAD	cpe (kN)	A (m2)	LOAD	cpe (kN)
1	1.13	F	-0.35748	0.904	G	-0.25808	1	1.13	J	-1.0313	0.904	I	-0.66461
2	1.016	F	-0.32142	0.837	G	-0.23896	2	1.016	J	-0.92725	0.837	I	-0.61535
3	0.962	F	-0.30433	0.77	G	-0.21983	3	0.962	J	-0.87797	0.77	I	-0.56609
4	0.879	H	-0.09495	0.703	H	-0.07594	4	0.879	J	-0.80222	0.703	I	-0.51683
5	0.795	H	-0.08588	0.636	H	-0.0687	5	0.795	J	-0.72556	0.636	I	-0.46758
6	0.711	H	-0.07681	0.569	H	-0.06147	6	0.711	J	-0.6489	0.569	I	-0.41832
7	0.628	H	-0.06784	0.502	H	-0.05423	7	0.628	J	-0.57315	0.502	I	-0.36906
8	0.544	H	-0.05877	0.435	H	-0.04699	8	0.544	J	-0.49648	0.435	I	-0.31981
9	0.46	H	-0.04969	0.368	H	-0.03975	9	0.46	J	-0.41982	0.368	I	-0.27055
10	0.377	H	-0.04073	0.301	H	-0.03252	10	0.377	J	-0.34407	0.301	I	-0.22129
11	0.293	H	-0.03165	0.234	H	-0.02528	11	0.293	J	-0.26741	0.234	I	-0.17203
12	0.209	H	-0.02258	0.167	H	-0.01804	12	0.209	J	-0.19074	0.167	I	-0.12278
13	0.126	H	-0.01361	0.1	H	-0.0108	13	0.126	J	-0.11499	0.1	I	-0.07352
14	0.042	H	-0.00454	0.033	H	-0.00356	14	0.042	J	-0.03833	0.033	I	-0.02426

A 7- Reactions of external pressures for θ=90º.

SIDE PARALEL TO WIND ACTION (L=15.5)									
	D1			D2		C			
	A (m2)	LOAD	cpe (kN)	LOAD	cpe (kN)		A (m2)	LOAD	cpe (kN)
1	1.838	L	-0.99274	N	-0.19855	1	1.016	N	-0.10975
2	1.702	L	-0.91928	N	-0.18386	2	1.016	N	-0.10975
3	1.566	L	-0.84583	N	-0.16917	3	1.016	N	-0.10975
4	1.429	L	-0.77183	N	-0.15437	4	1.016	N	-0.10975
5	1.293	L	-0.69838	N	-0.13968	5	1.016	N	-0.10975
6	1.157	L	-0.62492	N	-0.12498	6	1.016	N	-0.10975
7	1.021	L	-0.55146	N	-0.11029	7	1.016	N	-0.10975
8	0.885	L	-0.47801	N	-0.0956	8	1.016	N	-0.10975
9	0.749	L	-0.40455	N	-0.08091	9	1.016	N	-0.10975
10	0.613	L	-0.33109	N	-0.06622	10	1.016	N	-0.10975
11	0.476	L	-0.2571	N	-0.05142	11	1.016	N	-0.10975
12	0.34	L	-0.18364	N	-0.03673	12	1.016	N	-0.10975
13	0.204	L	-0.11018	N	-0.02204	13	1.016	N	-0.10975
14	0.068	L	-0.03673	N	-0.00735	14	1.016	N	-0.10975

A 8- Final reactions introduced in the software for θ=0º.

COMB θ=0º EXTERNAL										
	1	2	3	4	5	6	7	8	9	10
	DW +D1	D1+C	C+C	C+D2	D2+DL	DL+CL	CL+CL	CL+DL	DW+CW	CW+CW
	Cpe	Cpe	Cpe	Cpe	Cpe	Cpe	Cpe	Cpe	Cpe	Cpe
1	-1.19	-0.83	-0.45	-0.50	-0.95	-1.08	-0.83	-1.08	-0.87	-0.58
2	-1.10	-0.77	-0.41	-0.46	-0.88	-1.03	-0.83	-1.03	-0.83	-0.58
3	-1.02	-0.71	-0.38	-0.43	-0.81	-0.98	-0.83	-0.98	-0.79	-0.58
4	-0.63	-0.65	-0.35	-0.39	-0.74	-0.71	-0.38	-0.71	-0.26	-0.22
5	-0.57	-0.59	-0.31	-0.35	-0.67	-0.66	-0.38	-0.66	-0.25	-0.22
6	-0.51	-0.52	-0.28	-0.32	-0.60	-0.61	-0.38	-0.61	-0.23	-0.22
7	-0.45	-0.46	-0.25	-0.28	-0.53	-0.56	-0.38	-0.56	-0.22	-0.22
8	-0.39	-0.40	-0.21	-0.24	-0.46	-0.51	-0.38	-0.51	-0.21	-0.22
9	-0.33	-0.34	-0.18	-0.20	-0.39	-0.46	-0.38	-0.46	-0.19	-0.22
10	-0.27	-0.28	-0.15	-0.17	-0.32	-0.41	-0.38	-0.41	-0.18	-0.22
11	-0.21	-0.22	-0.12	-0.13	-0.24	-0.36	-0.38	-0.36	-0.16	-0.22
12	-0.15	-0.15	-0.08	-0.09	-0.17	-0.31	-0.38	-0.31	-0.15	-0.22
13	-0.09	-0.09	-0.05	-0.06	-0.11	-0.26	-0.38	-0.26	-0.13	-0.22
14	-0.03	-0.03	-0.02	-0.02	-0.04	-0.21	-0.38	-0.21	-0.12	-0.22

A 9- Final reactions introduced in the software for θ=90º.

COMB θ=90º EXTERNAL									
	1	2	3	4	5	6	7	8	9
	DW+D1	D1+C	C+C	C+D2	D2+DL	DL+CL	CL+CL	DW+CW	CW+CW
	Cpe	Cpe	Cpe	Cpe	Cpe	Cpe	Cpe	Cpe	Cpe
1	-1.35	-1.10	-0.22	-0.31	-1.23	-1.70	-1.33	-0.62	-0.52
2	-1.24	-1.03	-0.22	-0.29	-1.11	-1.54	-1.23	-0.56	-0.48
3	-1.15	-0.96	-0.22	-0.28	-1.05	-1.44	-1.13	-0.52	-0.44
4	-0.87	-0.88	-0.22	-0.26	-0.96	-1.32	-1.03	-0.17	-0.15
5	-0.78	-0.81	-0.22	-0.25	-0.87	-1.19	-0.94	-0.15	-0.14
6	-0.70	-0.73	-0.22	-0.23	-0.77	-1.07	-0.84	-0.14	-0.12
7	-0.62	-0.66	-0.22	-0.22	-0.68	-0.94	-0.74	-0.12	-0.11
8	-0.54	-0.59	-0.22	-0.21	-0.59	-0.82	-0.64	-0.11	-0.09
9	-0.45	-0.51	-0.22	-0.19	-0.50	-0.69	-0.54	-0.09	-0.08
10	-0.37	-0.44	-0.22	-0.18	-0.41	-0.57	-0.44	-0.07	-0.07
11	-0.29	-0.37	-0.22	-0.16	-0.32	-0.44	-0.34	-0.06	-0.05
12	-0.21	-0.29	-0.22	-0.15	-0.23	-0.31	-0.25	-0.04	-0.04
13	-0.12	-0.22	-0.22	-0.13	-0.14	-0.19	-0.15	-0.02	-0.02
14	-0.04	-0.15	-0.22	-0.12	-0.05	-0.06	-0.05	-0.01	-0.01